Outflow Tract Anomalies

13

Nadine Choueiter, Roque Ventura, and Leo Lopez

Abbreviations

3D	Three-dimensional
AoV	Aortic valve
AR	Aortic regurgitation
AS	Aortic stenosis
CHD	Congenital heart disease
CT	Computed tomography
DCRV	Double chamber right ventricle
EROA	Effective regurgitant orifice area
LV	Left ventricle
LVOT	Left ventricular outflow tract
MRI	Magnetic resonance imaging
PISA	Proximal isovelocity surface area
PR	Pulmonary regurgitation
PS	Pulmonary stenosis
PV	Pulmonary valve
RV	Right ventricle
RVOT	Right ventricular outflow tract
TEE	Transesophageal echocardiography
VSD	Ventricular septal defect

Key Learning Objectives

- Identify congenital and acquired structural lesions of the left ventricular outflow tract on transesophageal echocardiography (TEE)
- Know how to perform pre and postoperative evaluation of the left ventricular outflow tract on TEE
- Identify congenital and acquired structural lesions of the right ventricular outflow tract on TEE
- Know how to perform pre and postoperative evaluation of the right ventricular outflow tract on TEE

Introduction

Anomalies of the outflow tracts are usually associated with obstruction, regurgitation, and/or aneurysmal dilation of the proximal great arteries. Based on an analysis of almost 40 published articles on the incidence of congenital heart disease spanning many decades, pulmonary stenosis (PS), the most common anomaly of the right ventricular outflow tract (RVOT), ranks as the fourth most common congenital heart disease (CHD) with a mean incidence of 0.73 per 1000 live births, and aortic stenosis (AS), the most common anomaly of the left ventricular outflow tract (LVOT), ranks as the seventh most common with a mean incidence of 0.40 per 1000 live births [1]. Among almost 60,000 patients evaluated at the Cardiovascular Program of Children's Hospital Boston from 1988 to 2002, a pulmonary valve (PV) abnormality was the fourth most common diagnosis with a frequency of 5.7%, and an aortic valve (AoV) abnormality was the fifth most common with a frequency of 5.5% [2]. A bicuspid AoV is in fact the most common CHD with an incidence of 0.4% to 2% in the general population [3–5]. Because isolated obstruction at the valvar level in both outflow tracts is generally treated in the catheterization laboratory rather than in the operating room, intraoperative transesophageal echocardiography (TEE) is not frequently performed for

Electronic Supplementary Material The online version of this chapter (https://doi.org/10.1007/978-3-030-57193-1_13) contains supplementary material, which is available to authorized users.

N. Choueiter (✉)
The Pediatric Heart Center, Children's Hospital at Montefiore, New York, NY, USA
e-mail: nchoueit@montefiore.org

R. Ventura
Miami Children's Hospital, Miami, FL, USA

L. Lopez
Betty Irene Moore Children's Heart Center, Lucile Packard Children's Hospital, Stanford University School of Medicine, Palo Alto, CA, USA

P. C. Wong, W. C. Miller-Hance (eds.), *Transesophageal Echocardiography for Pediatric and Congenital Heart Disease*,
https://doi.org/10.1007/978-3-030-57193-1_13

valvar stenosis. However, if the obstruction occurs at the subvalvar or supravalvar level or if the primary lesion is regurgitation and/or aneurysmal dilation of the proximal great artery, surgical intervention is often necessary, thereby requiring intraoperative TEE before and after the surgery.

Utility of Transesophageal Echocardiography

Patients with significant outflow tract anomalies other than valvar AS or PS do not usually require surgery during the first year of life, and they often do not undergo any intervention until they are toddlers, adolescents, or adults. Outflow tract obstruction and semilunar valve regurgitation are usually associated with a morphologic abnormality at or near the semilunar valves. During the preoperative evaluation in the operating room, TEE can generally provide information regarding the morphology of the outflow tracts in the midesophageal and upper esophageal views, as well as the degree of obstruction and regurgitation, if present, in the deep transgastric (Fig. 13.1, Videos 13.1a and 13.1b) and midesophageal views [6]. (see Chap. 4) Postoperative TEE can evaluate the success of a surgical procedure and exclude residual obstruction, regurgitation, or other potential complications. It is important to note that TEE data will always reflect the patient's hemodynamics, which can be affected by general anesthesia, inotropic support, volume status, and ventricular function (see Chap. 18). For example, the degree of residual obstruction or regurgitation across a semilunar valve can be underestimated in the setting of general anesthesia, hypovolemia, tachycardia, or poor ventricular function. In contrast, the degree of dynamic obstruction, as seen in tetralogy of Fallot or hypertrophic cardiomyopathy secondary to muscular hypertrophy in the subarterial region, can be overestimated with hypovolemia or hyperdynamic ventricular function, especially with inotropic support [7]. Occasionally, TEE is necessary outside of the operating room for older patients with poor transthoracic echocardiographic windows, particularly if the patient has undergone prior surgery.

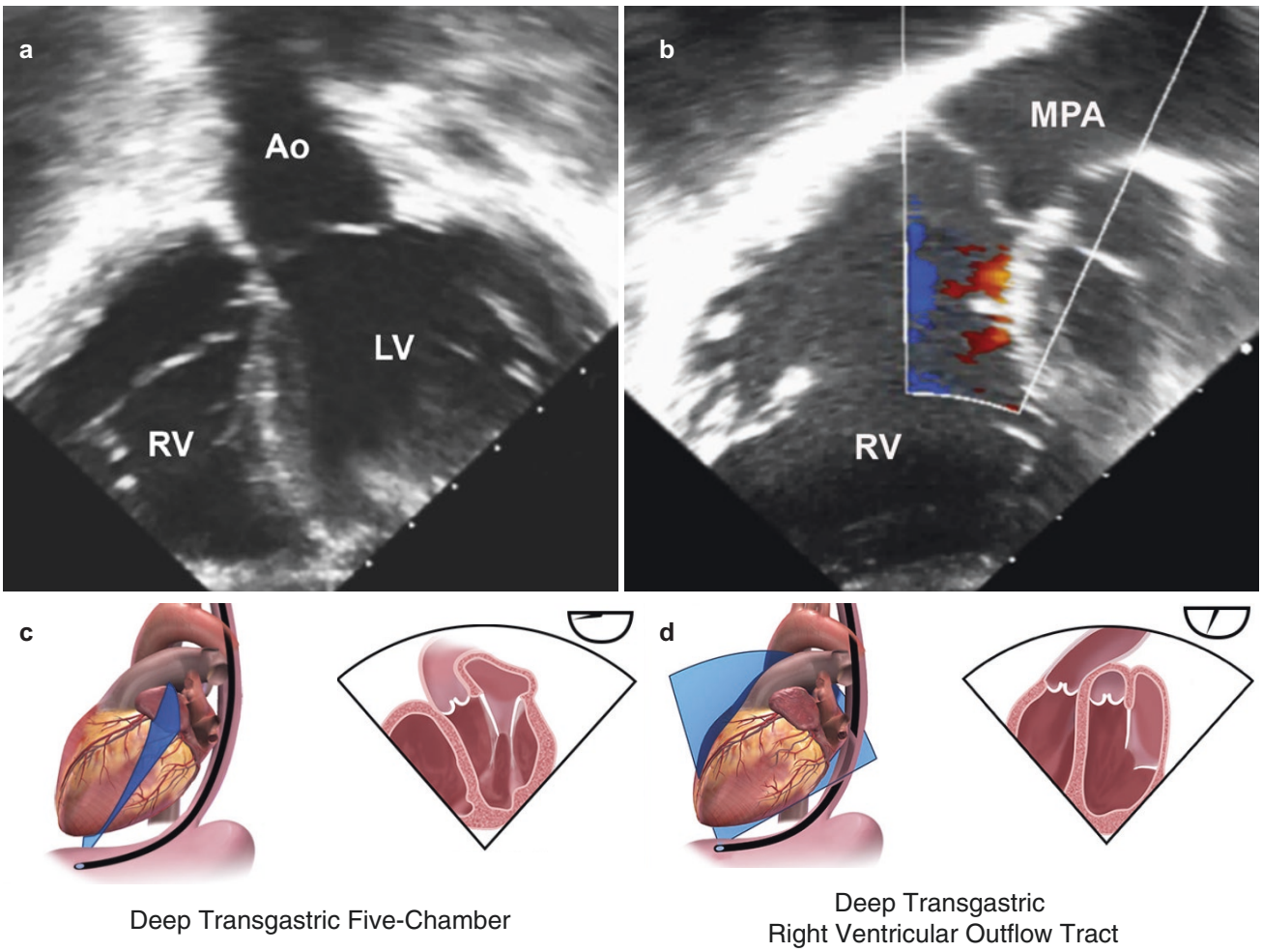

Fig. 13.1 (**a**) Deep transgastric five-chamber (DTG 5-Ch) view at 0° showing the left ventricular outflow tract. (**b**) Deep transgastric right ventricular outflow tract (DTG RVOT) view at 80°-90°. This view opens the entire right ventricular outflow tract. (**c**) Illustration depicting how the left ventricular outflow tract is evaluated using the DTG 5-Ch view. (**d**) Illustration depicting how the right ventricular outflow tract is evaluated using the DTG RVOT view. (*Ao* aorta, *LV* left ventricle, *MPA* main pulmonary artery, *RV* right ventricle). (**c**) and (**d**) from Pulchalski et al. [6], used with permission from Elsevier

Normal Anatomy

The term conotruncus (from the Greek words conus for cone and truncus for trunk or body) represents the outflow tracts of both ventricles. It is composed of the subarterial regions, the semilunar valves, the great arterial roots, and the proximal trunks. The conus (also known as the infundibulum from the Latin word for funnel) defines the subarterial muscular chamber, which prevents fibrous continuity between a semilunar valve and the corresponding atrioventricular valve. In the normal heart, the subpulmonary conus prevents fibrous continuity between the tricuspid valve and the PV. The supraventricular crest is the prominent muscular shelf along the posterior aspect of the subpulmonary conus, and it is composed of the right ventriculo-infundibular fold separating the tricuspid valve leaflets from the PV leaflets, the subpulmonary muscular sleeve supporting the PV leaflets, and the conal septum (or infundibular septum) separating the RVOT from the LVOT (though its presence in the normal heart has been a source of controversy). The subpulmonary conus is separated from the trabecular segment of the right ventricular chamber at the infundibular os, an area defined by the moderator band, the septal band (also known as the septomarginal trabeculation), and the parietal band of the right ventricle (RV). The subaortic conus regresses *in utero*, resulting in varying degrees of fibrous continuity between the mitral valve and AoV. This fibrous area, known as the mitral-aortic intervalvular fibrosa, is measured as the shortest distance from the hinge of the anterior mitral leaflet to the base of the non-coronary or left coronary AoV leaflet, and it can be elongated in cases of subvalvar AS and tetralogy of Fallot.

The normal semilunar valve is a three-dimensional (3D) structure where three leaflets or cusps are attached to the arterial root and supporting ventricular muscle in a semilunar or crown-like fashion. The leaflets are separated by three commissures that extend during diastole from the center of the valve at the level of the ventriculo-arterial junction to the periphery at the level of the sinotubular junction (Fig. 13.2, Video 13.2). It is important to recognize that the semilunar "annulus" is in fact a diagnostician construct without a true anatomic correlate since the semilunar valve leaflet attachments extend from the anatomic ventriculo-arterial junction up to the sinotubular junction; the so-called "annulus" as defined in echocardiography represents only the most proximal attachments of the semilunar valve and not the attachments in their entirety [8] (Fig. 13.3, Video 13.3).

Left Ventricular Outflow Tract Anomalies

Valvar Aortic Stenosis

Congenital valvar AS results from a bicuspid or unicuspid AoV, a dysplastic tricuspid AoV, or a hypoplastic aortic "annulus". Acquired valvar AS usually results from calcification secondary to degenerative or post-inflammatory causes [9], though a bicuspid AoV is also a risk factor for calcification [5]. A bicus-

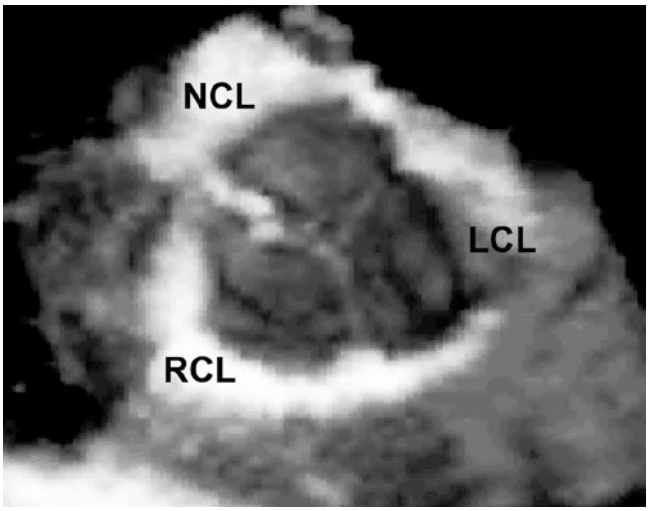

Fig. 13.2 Three-dimensional TEE *en face* view obtained from the midesophageal aortic valve short axis, depicting the three-dimensional nature of a normal trileaflet aortic valve (*LCL* left coronary leaflet, *NCL* non-coronary leaflet, *RCL* right coronary leaflet)

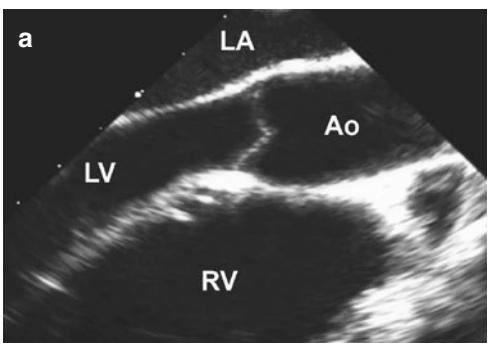

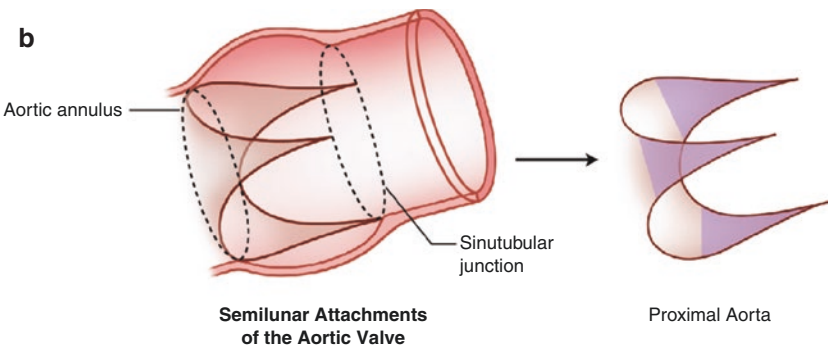

Fig. 13.3 (**a**) Midesophageal aortic valve long axis view at 120° showing the left ventricular outflow tract. (**b**) Illustration of the aortic valve and its semilunar attachments within the aortic root from the ventriculo-arterial junction to the sinotubular junction (*Ao* aorta, *LA* left atrium, *LV* left ventricle, *RV* right ventricle)

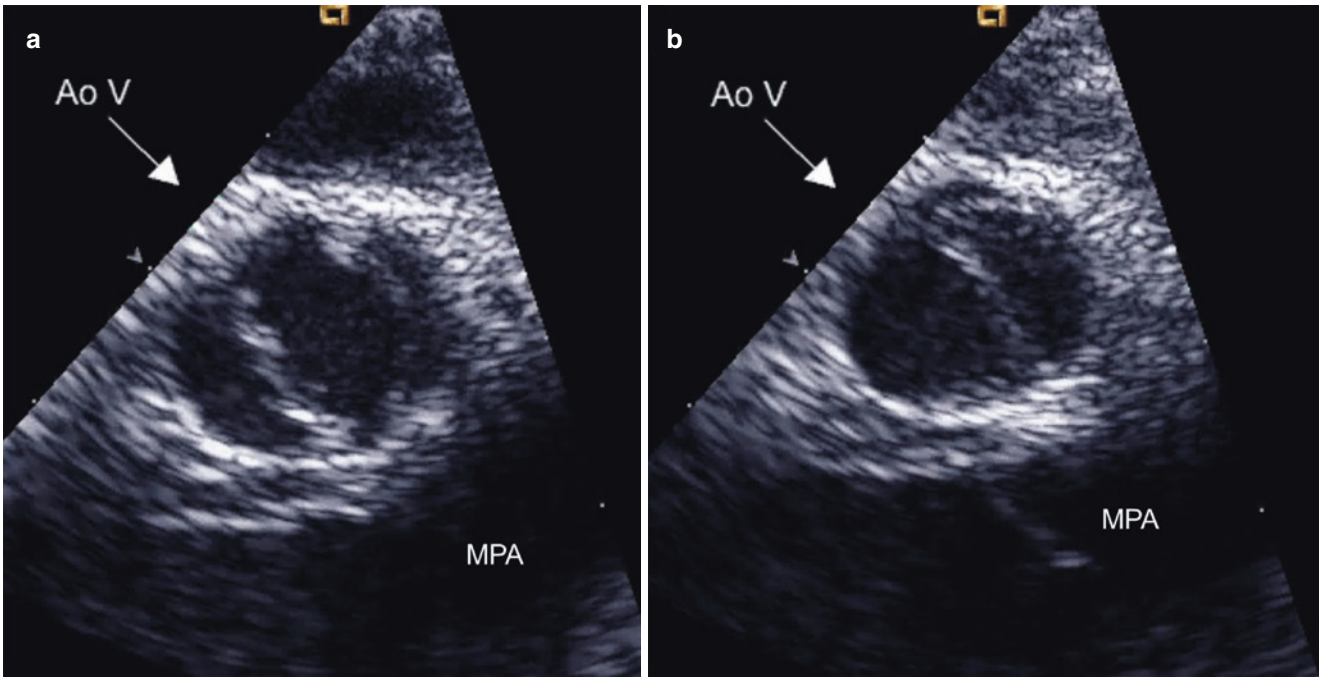

Fig. 13.4 Midesophageal aortic valve short axis view at 30° shows a true bicuspid aortic valve (*AoV*) with only two leaflets (the right and left coronary leaflets) and absent non-coronary leaflet, in the open (**a**) and closed (**b**) positions. This gives a "fish mouth" appearance to the valve orifice (*MPA* main pulmonary artery)

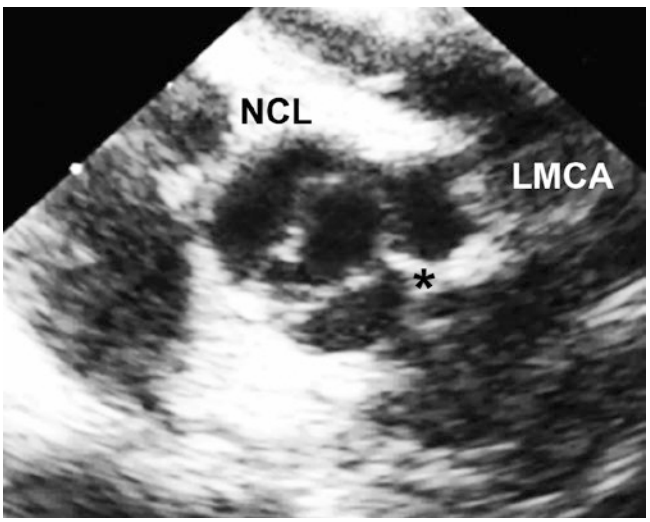

Fig. 13.5 Midesophageal aortic valve short axis view at 30° showing a bicuspid aortic valve with fusion or underdevelopment of the intercoronary commissure between the left and right coronary leaflets (black asterisk) (*NCL* non-coronary leaflet, *LMCA* left main coronary artery)

Fig. 13.6 Midesophageal aortic valve short axis view at 30° showing a bicuspid aortic valve with fusion or underdevelopment of the commissure between the right and non-coronary leaflets (black asterisk) (*LCL* left coronary leaflet)

pid AoV is the most common cause of valvar AS, although the presence of a bicuspid AoV does not necessarily mean a patient has (or will develop) valvar AS. As noted previously, a bicuspid AoV is the most common congenital heart defect, with an incidence of 0.4% to 2% in the general population [3–5]. There are several distinct anatomic variations. It is rare to encounter a bicuspid AoV with only two well-developed leaflets instead of three (Fig. 13.4, Video 13.4); instead, it usually involves fusion of two of the three leaflets or underdevelopment of one of the commissures (known as a raphe) [10]. It is because of the absence of one of the three commissures that the lesion is often referred to as a bicommissural AoV. Among these, fusion occurs most commonly at the intercoronary commissure between the right and left coronary leaflets with a frequency of 70% (Fig. 13.5, Video 13.5), followed by the commissure between the right and non-coronary leaflets with a frequency of 28% (Fig. 13.6, Video 13.6); fusion at the commissure between the left and non-coronary leaflets is very rare [11]. In adults, the rate of AS progression appears to be higher in those valves with

fusion of the intercoronary commissure [12], although studies in children have revealed more rapid progression of AS and regurgitation as well as shorter time from diagnosis to intervention in valves with fusion of the commissure between the right and non-coronary leaflets [13]. Associations with a bicuspid AoV include aortic coarctation [3] or interrupted aortic arch, subvalvar AS, a ventricular septal defect (VSD), a coronary anomaly, Turner syndrome [14], and aortic dilation or aneurysm formation [15–17]. Valvar AS can be progressive, and the degree of progression may be associated with age at presentation and/or severity at the time of presentation [18]. Although it occurs rarely, sudden death in this patient population appears to be related to significant stenosis and regurgitation [19]. In addition, the chronic pressure load experienced by the left ventricle (LV) leads to hypertrophy with the potential for permanent muscular damage and fibrosis. Therefore, management of these patients must focus on prevention of these sequelae.

Over the past several decades, transcatheter balloon valvotomy in the catheterization laboratory has become a more popular management approach for patients with valvar AS, superseding surgical valvotomy as the primary mode of treatment. TEE is not often needed during either of these procedures, though occasionally it is helpful in determining the appropriate intervention and/or assessing its efficacy. TEE for valvar AS should always include assessment of the leaflets and commissural morphology, degree of obstruction, degree of LV hypertrophy, ascending aortic size, and left atrial dilation. Leaflets and commissural morphology are best evaluated in the midesophageal views, usually at 25° to 45° for the midesophageal aortic valve short axis (ME AoV SAX) images (Figs. 13.4, 13.5, 13.6, and 13.7, Videos 13.4, 13.5, 13.6, and 13.7) and at 90° ~ 120° for the midesophageal aortic valve long axis (ME AoV LAX) images (Fig. 13.8, Video 13.8). The midesophageal five-chamber (ME 5-Ch) view at 0°–10° is also useful for evaluating the aortic valve and LV outflow tract. It is, however, important to recognize that pure short and long axis images are not always available by TEE because of the fixed spatial relationship between the esophagus and the aortic outflow tract. When a pure short axis image is available (that is, when the AoV annular plane is completely parallel to the axis of the ultrasonic beam), the relative sizes of the leaflets should be evaluated, and failure of commissural opening in the setting of a bicuspid or unicuspid valve can be displayed. Long axis imaging of the AoV (that is, when the AoV annular plane is 90° to the plane of the ultrasonic beam) can reveal thickened and doming leaflets. Three-dimensional echocardiography has emerged as an important tool for the assessment of aortic valve anatomy and pathology (Chaps. 23 and 24).

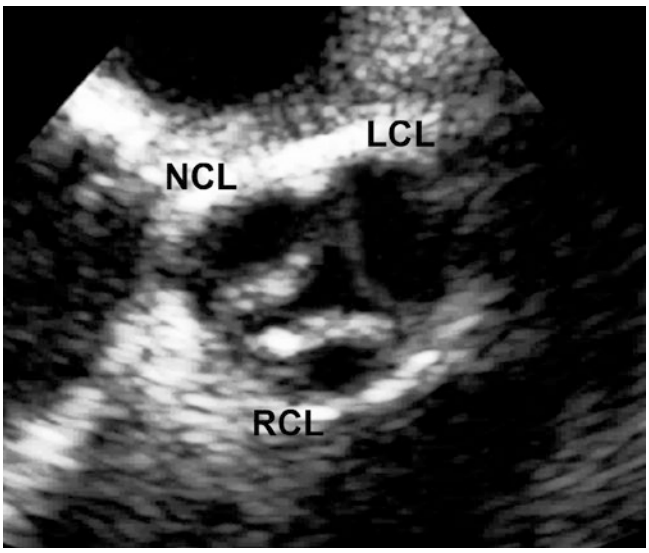

Fig. 13.7 Midesophageal aortic valve short axis view at 30° showing a dysplastic aortic valve with thickened right and non-coronary leaflets (*LCL* left coronary leaflet, *NCL* non-coronary leaflet, *RCL* right coronary leaflet)

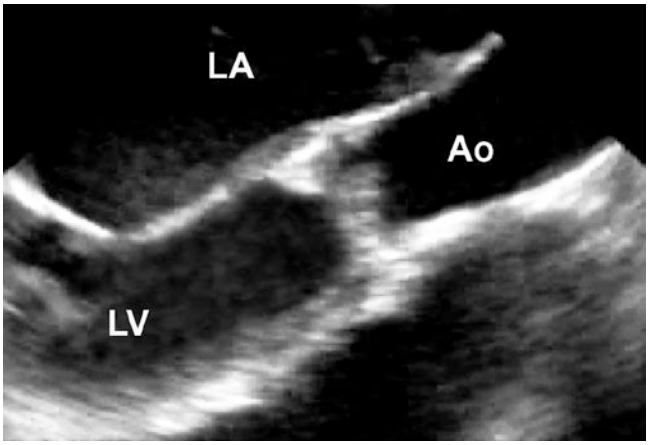

Fig. 13.8 Midesophageal aortic valve long axis view at 120° showing a dysplastic aortic valve associated with valvar aortic stenosis (*Ao* aorta, *LA* left atrium, *LV* left ventricle)

The degree of obstruction is generally assessed by continuous wave Doppler interrogation along the aortic outflow tract, and this is best performed in the deep transgastric five-chamber (DTG 5-Ch) view with transducer angle between 0°–30° (Fig. 13.1a, Video 13.1a), or sometimes from the deep transgastric right ventricular outflow tract (DTG RVOT) view with transducer angle between 80°–110° (Fig. 13.1b, Video 13.1b). Because of the distance from the probe to the outflow tract, imaging from this view often requires using the lowest possible frequency for improved penetration as well as minimizing the image and color sector size. Every effort should be made to align the Doppler beam with the LVOT. As an alternative, the transgastric long axis view (TG LAX) can be used for interrogation of the LVOT because it generally provides favorable angles for continuous wave Doppler interrogation (Chap. 4) with a shorter distance from the probe to the aortic valve. Both peak and mean pressure gradients should be measured [20–22]. It is important to recognize that echocardiography-derived Doppler gradients often do not correspond to the

peak-to-peak gradient measured in the catheterization laboratory, a common discrepancy which results from several factors, including a phenomenon called pressure recovery [23]. In addition, severe LV dysfunction in the setting of valvar AS is associated with low cardiac output and diminished transvalvar flow, and Doppler interrogation may reveal a low gradient despite severe obstruction at the valvar level. Similarly, the degree of LVOT obstruction can be artificially decreased in the setting of general anesthesia, deep sedation, or hypovolemia. In addition to pressure gradient, some use calculated aortic valve area to evaluate the degree of obstruction as derived by the *continuity equation*, which states that the stroke volume in the subaortic region is the same as the stroke volume at the valvar level (see Chap. 1). Since stroke volume is equal to the velocity-time integral multiplied by cross-sectional area at a particular location, the effective aortic valve area can be calculated if the LVOT cross-sectional area and the velocity-time integrals at the LVOT and at the aortic valve are known [24]. However, the LVOT is frequently not circular in shape, precluding accurate assessment of LVOT cross-sectional areas using LVOT diameters, and some have suggested that 3D TEE may be preferable to two-dimensional imaging for more accurate assessments of aortic valve area [25].

It is important to note that AS represents a disease continuum, and severity cannot be defined by a single value [22]. With these considerations in mind, the following echocardiographic criteria for classification of AoV stenosis severity were given by a 2014 American College of Cardiology/American Heart Association (ACC/AHA) Task Force on Valvular Heart Disease [22]:

- Mild: peak velocity < 3 m/s, mean gradient <20 mmHg, valve area > 1.5 cm^2
- Moderate: peak velocity 3.0–3.9 m/s, mean gradient 20–39 mmHg, valve area 1.0–1.5 cm^2
- Severe: peak velocity > 4 m/s, mean gradient >40 mmHg, valve area < 1.0 cm^2

Similar guidelines have not been written specifically for the pediatric population. At present, the above criteria are generally applied to this group of patients as well [26–28]. LV hypertrophy is best evaluated in the transgastric basal short-axis (TG Basal SAX) and transgastric mid papillary short axis (TG Mid Pap SAX) views at 0°, though a quantitative assessment of the degree of hypertrophy may not be reliable with TEE, again because pure short axis images of the LV in transgastric views at 0° may not always be available. The size of the aortic root and ascending aorta is best measured in midesophageal aortic valve long axis (ME AoV LAX) and midesophageal ascending aortic long axis (ME Asc Ao LAX) views at 90°–120°; important measurements that should be obtained in early to mid-systole include the diameters of the aortic valve annulus, aortic root, sinotubular junction, and ascending aorta [29]. These measurements are analogous to those obtained by transthoracic echocardiography, and they can be compared to published normal values [30, 31]. Left atrial dilation can be easily visualized in midesophageal four-chamber (ME 4-Ch) and two-chamber (ME 2-Ch) views at transducer angles of 0° and 90° respectively.

Over the last decade, transcatheter AoV replacement/implantation, or TAVR/TAVI, has emerged as a non-surgical treatment for severe valvar AS (also see Chap. 21). It is performed in the cardiac catheterization laboratory and involves the implantation of a bovine or porcine pericardial valve mounted upon a metal support frame [32, 33]. Delivered transarterially (access by percutaneous femoral or subclavian artery, or through the LV apex), the balloon-mounted valve is advanced to the AoV position, and the balloon expanded within the AoV, displacing the diseased native valve leaflets. During the procedure, TEE is utilized and serves a number of important functions: (a) pre-procedure evaluation of anatomy and function; (b) monitoring of valve implantation; (c) post-implantation evaluation of valve function and valve regurgitation (Fig. 13.9, Video 13.9). The post-implantation TEE is particularly useful in that it enables accurate differentiation between transvalvar and paravalvar aortic regurgitation, something not easily visualized by angiography or fluoroscopy [34]. At present, two major valves are available—the Edwards SAPIEN 3 heart valve (Edwards Lifesciences Inc., Irvine, California) and the Evolut Pro (CoreValve) system (Medtronic Inc., Minneapolis, Minnesota)—but a number of other valves are undergoing early clinical evaluation [35]. While originally reserved for high risk adults with severe aortic stenosis [36–38], the recent PARTNER 3 trial demonstrated favorable outcomes with the SAPIEN 3 valve in low-risk patients with severe aortic valve stenosis [39].

Subvalvar Aortic Stenosis

Subvalvar AS is rarely diagnosed *in utero* or in the newborn period, prompting many people to classify this lesion as an acquired heart disease rather than a congenital one [40, 41]. It is a progressive disease, particularly in children, and some have suggested that its development might involve the following mechanisms: abnormal LVOT morphology leads to increased septal shear stress, which because of some genetic predisposition leads in turn to cellular proliferation [42, 43]. Some of the abnormalities in LVOT morphology that are associated with subvalvar AS include a steep aorto-septal angle (Fig. 13.10a, Video 13.10), an elongated mitral-aortic intervalvular fibrosa, exaggerated aortic override [44, 45] prominent LVOT muscle bundles, and abnormal mitral valve attachments to the ventricular septum. In addition, the distance from the level of the obstruction to the AoV appears to be one of the major predictors of significantly progressive obstruction [46] (Fig. 13.10b, Video 13.10). Subvalvar AS can occur with or without a VSD. Examples of subvalvar AS in the absence of

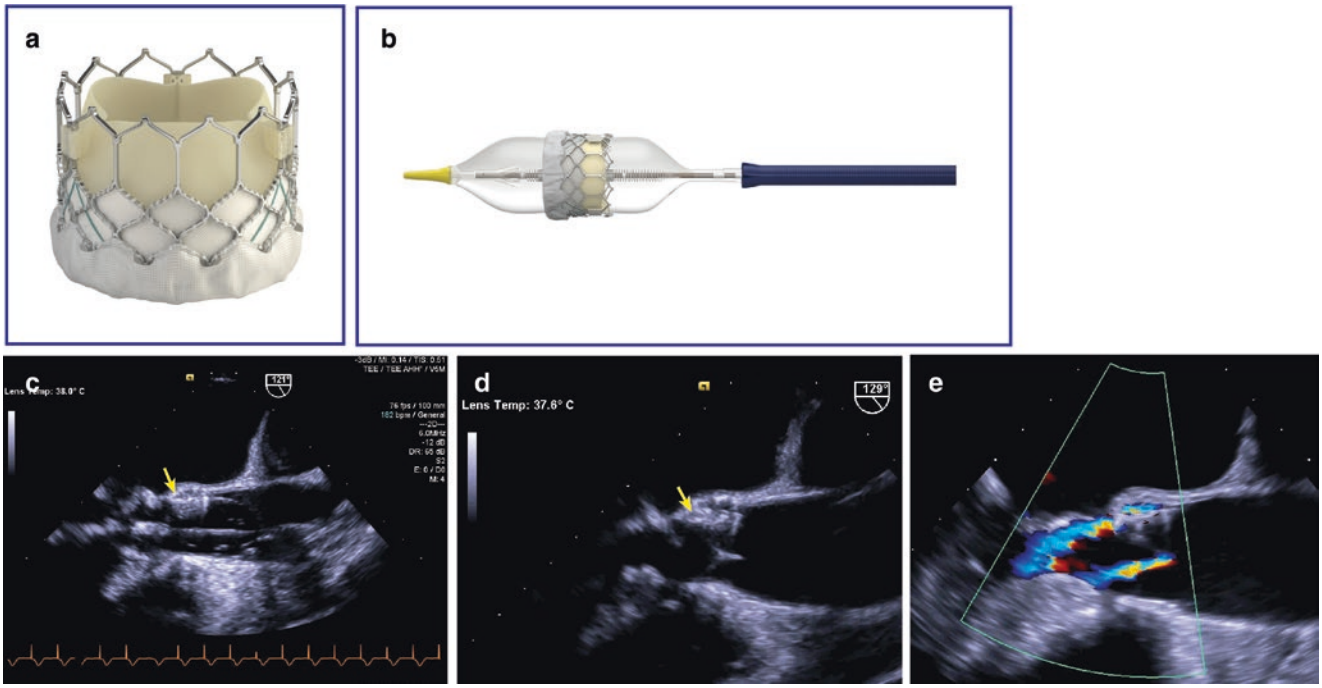

Fig. 13.9 Transcatheter aortic valve replacement/implantation (TAVR/TAVI). (**a**) Shows the Edwards SAPIEN 3 valve (Edwards Lifesciences Inc., Irvine, California), a bovine pericardial valve mounted on a balloon expandable cobalt-chromium frame. (**b**) Shows the same valve mounted on a balloon catheter that is used for valve delivery. (**c–e**) are transesophageal echocardiographic images obtained from the mid-esophageal aortic valve long axis view at 120°-130°. (**c**) Shows the balloon being inflated (device indicated with arrow), and (**d**) Shows the valve (arrow) after implantation. In (**e**), following valve implantation color flow Doppler shows two small jets of regurgitation: one a central transvalvular jet, the other a peripheral paravalvular jet

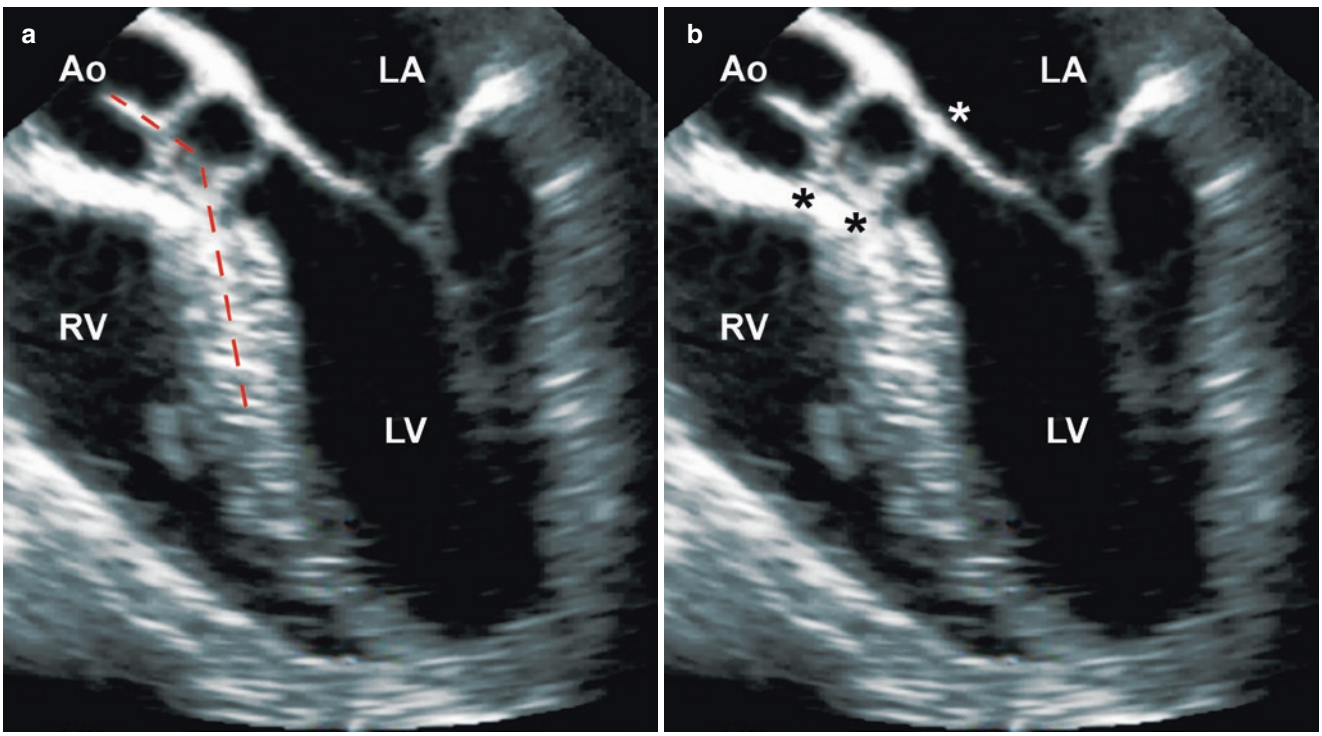

Fig. 13.10 Midesophageal five-chamber view with probe anteflexion to visualize the left ventricular outflow tract, showing a subaortic fibromuscular ridge associated with subvalvar aortic stenosis. The two figures depict (**a**) a steep aortoseptal angle (*dashed red lines*), and (**b**) the distance between the ridge and the aortic annulus (*black asterisk*) and extension of the fibromuscular ridge to the anterior mitral leaf-let (*white asterisk*) (*Ao* aorta, *LA* left atrium, *LV* left ventricle, *RV* right ventricle)

a VSD include: (a) a discrete fibrous or fibromuscular subaortic ridge protruding from the ventricular septum and sometimes extending to the anterior mitral leaflet (Fig. 13.10b, Video 13.10); (b) an extensive muscular shelf creating a tunnel-like LVOT; (c) hypertrophic cardiomyopathy with dynamic obstruction secondary to diffuse septal hypertrophy and systolic anterior motion of the mitral valve and/or its tensor apparatus. Subvalvar AS without a VSD can also develop postoperatively after mitral valve replacement with a mechanical prosthesis [47–49]. The most common type of subvalvar AS in the setting of a VSD occurs with posterior deviation of the conal septum, a lesion that is often associated with aortic coarctation or interrupted aortic arch [50, 51] (see Chap. 16). Other examples include endocardial folds or fibromuscular ridges at the crest of the muscular septum, often without significant obstruction [52], and abnormal mitral valve attachments to the ventricular septum, often in the setting of an atrioventricular canal (atrioventricular septal) defect (see Chap. 8) Aside from a VSD, subvalvar AS can also be associated with a bicuspid AoV, a double chamber RV (DCRV) [53], and aortic regurgitation (AR). In fact, the risk for rapidly progressive AR is frequently the reason that children with subvalvar AS require early surgical intervention [54], although AR in adults with subvalvar AS is rarely progressive [55, 56].

Preoperatively, TEE is especially useful in delineating the mechanism of obstruction in patients with subvalvar AS. A fibromuscular ridge with or without extension to the anterior mitral leaflet, posterior deviation of the conal septum, a tunnel-like LVOT, and abnormal mitral valve attachments to the ventricular septum can usually be characterized in the ME 4-Ch, ME 5-Ch (Fig. 13.10, Video 13.10), and ME AoV LAX (at ~120°) views (Fig. 13.11, Video 13.11) or in the DTG 5-Ch view at 0°–30° and DTG RVOT view at 80–110°. In addition, the distance from a fibromuscular ridge to the AoV leaflets can be measured in these views (Fig. 13.10b). The degree of AR can usually be assessed in multiple midesophageal and deep transgastric views (as discussed later in this chapter). The AoV cusp and commissural morphology should always be evaluated in the ME AoV SAX view at ~30° (Figs. 13.4, 13.5, 13.6, and 13.7), especially in the setting of significant AR. The utility and limitations of the DTG 5-Ch view at 0°–30° in quantifying the degree of obstruction have been discussed previously. Occasionally a ME Asc Ao LAX view at ~120°, or higher view such as the upper esophageal aortic arch long axis (UE Ao Arch LAX) at 0° or upper esophageal aortic arch short axis (UE Ao Arch SAX) at ~70°–90° can provide an adequate Doppler angle to measure the gradient arising from the subaortic region. In some instances of subvalvar AS, a favorable angle for spectral Doppler interrogation can even be obtained from a modified ME 4-Ch view, though care must be taken not to contaminate the continuous wave Doppler tracing with a mitral regurgitation jet present along the same scan line. After mitral valve replacement with a mechanical prosthesis, the midesophageal window can be ineffective because the mechanical prosthesis is located between the TEE probe and the LVOT, and acoustic interference by the prosthesis can partially or completely inhibit visualization of the outflow tract. In these instances, the TG LAX and deep transgastric views

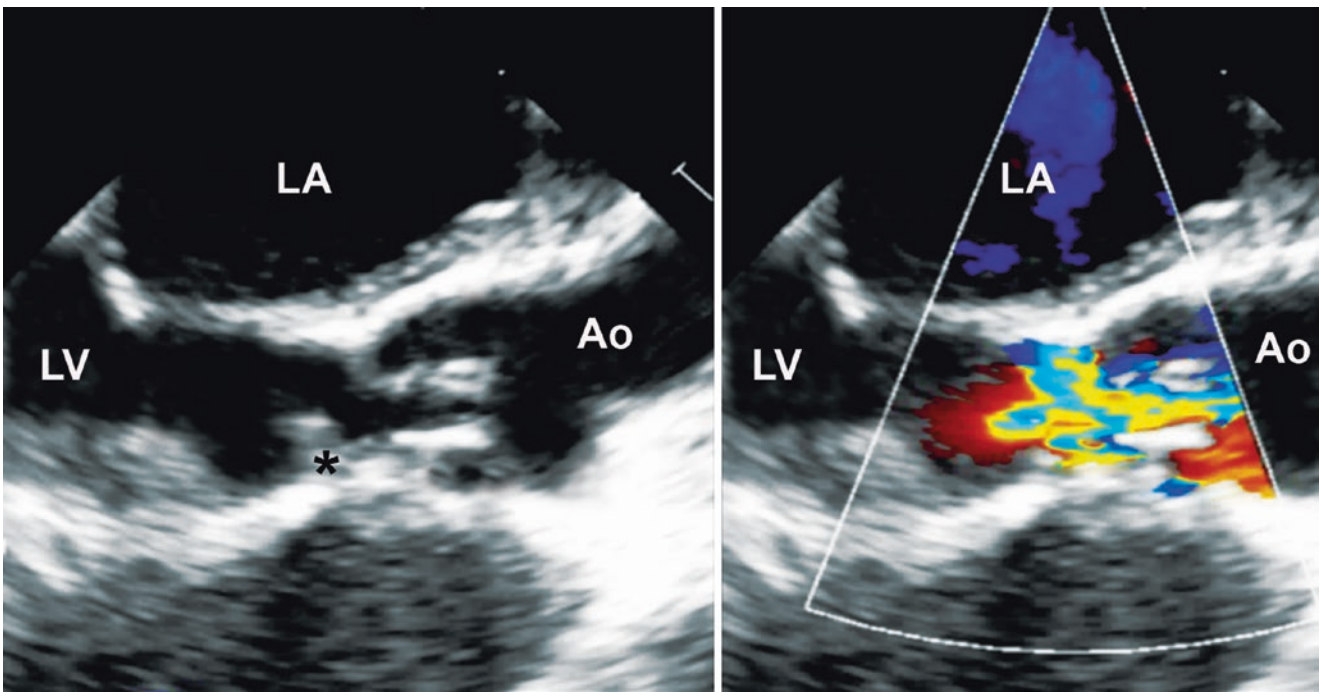

Fig. 13.11 Midesophageal aortic valve long axis view at 120° showing a subaortic fibromuscular ridge (*black asterisk*) and a dysplastic aortic valve resulting in combined subvalvar and valvar aortic stenosis in addition to a small membranous ventricular septal defect (not well-seen on the image, but readily visible on Video 13.12). The fibromuscular ridge is located at the crest of the muscular septum. (*Ao* aorta, *LA* left atrium, *LV* left ventricle)

(DTG 5-Ch, DTG RVOT) can be particularly useful since the probe is positioned beyond the prosthesis, allowing for unobstructed imaging and Doppler interrogation. Associations such as a VSD or a DCRV should be excluded, and these are usually visualized in the midesophageal views: the ME 4-Ch view at 0° and the midesophageal right ventricular inflow-outflow (ME RV In-Out) at 50°–70°. On the postoperative TEE, residual LVOT obstruction should be excluded qualitatively in the ME AoV LAX and midesophageal long axis (ME LAX) views (transducer angle for both at ~120°), and quantitatively in the DTG 5-Ch, DTG RVOT, and TG LAX views. The AoV leaflets should be re-evaluated in the ME AoV SAX view at 30°–45°, and the presence of post-interventional AR should be assessed in multiple midesophageal and deep transgastric views. Finally, inadvertent VSD creation and/or mitral valve injury are known complications following surgical intervention of subvalvar aortic stenosis [57–59]. See Chap. 10, Case Study #2 for an example of inadvertent VSD creation following subaortic stenosis resections. These areas should be evaluated carefully using a variety of midesophageal and deep transgastric views, as described above and in Chap. 4.

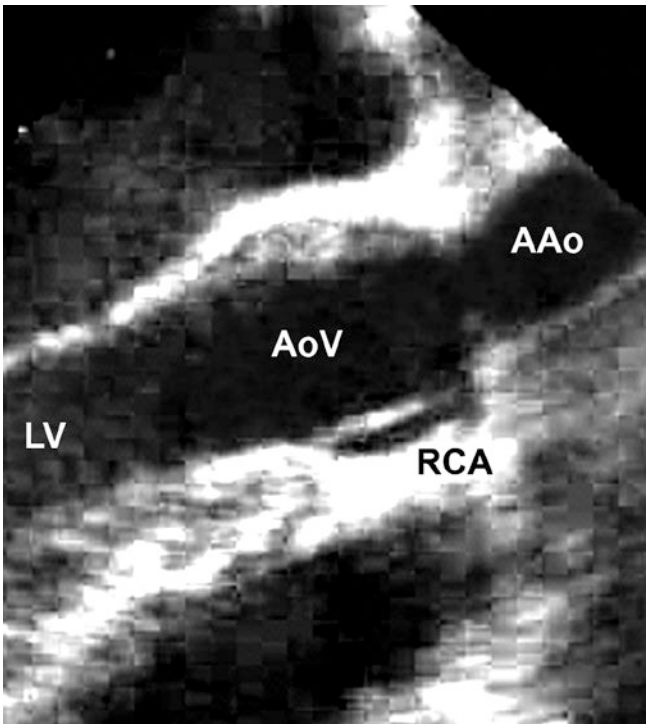

Fig. 13.12 Midesophageal aortic valve long axis view at 120° showing discrete narrowing at the sinotubular junction resulting in supravalvar aortic stenosis and entrapment of the right coronary ostium (*AAo* ascending aorta, *AoV* aortic valve, *LV* left ventricle, *RCA* right coronary artery)

Supravalvar Aortic Stenosis

Supravalvar AS is the least common type of LVOT obstruction, representing only 7% of all patients undergoing surgical repair for LVOT obstruction at Children's Hospital Boston from 1956 to 1976 [60]. Although it occasionally presents as a familial autosomal dominant lesion or as a sporadic idiopathic disorder, it is usually associated with Williams syndrome, a constellation of clinical features which include developmental delay, calcium metabolism problems, failure to thrive, and abnormal facial features [61]. Supravalvar AS results from a mutation or deletion of the elastin gene on chromosome 7 [62, 63]. The obstruction occurs at the sinotubular junction, and three anatomic subtypes have been described: the hourglass type (most common) involving dilation of the aortic root proximal to the narrowing and the ascending aorta distal to the narrowing (Fig. 13.12, Video 13.12), the membranous or diaphragmatic type, and the rare tubular type with diffuse hypoplasia of the ascending aorta [64, 65]. Patients with Williams syndrome can also have branch pulmonary artery stenosis, aortic coarctation, and renal artery stenosis in addition to supravalvar AS. Other associations include subvalvar AS, an abnormal AoV, and coronary abnormalities such as coronary artery dilation, coronary thickening, ostial stenosis, and ostial entrapment by a tethered AoV (Fig. 13.12). Obstruction can occur at more than one level, and the degree of obstruction usually progresses over time. Surgical intervention is generally undertaken when significant obstruction is present in order to prevent irreversible LV myocardial damage. In many cases, TEE is superior to transthoracic echocardiography in the evaluation of the entire extent of the ascending aorta. Preoperatively the aortic root and ascending aorta are best assessed by TEE in a ME 5-Ch view or ME AoV LAX view at ~120°, wherein the long axis of the proximal aorta can be displayed (Fig. 13.12, Video 13.12). During probe withdrawal in this view, the ascending aorta can be further evaluated with the ME Asc Ao LAX view. The degree of obstruction can be quantified with DTG 5-Ch (Fig. 13.13, Video 13.13), DTG RVOT, and TG LAX views. Occasionally, withdrawing the probe to an UE Ao Arch LAX or UE Ao Arch SAX view will provide an adequate Doppler angle of interrogation to quantify the degree of obstruction. The TEE examination (using two-dimensional imaging, color mapping, and Doppler interrogation) should also exclude other associations such as subvalvar AS (ME 4-Ch, ME AoV LAX views), an abnormal AoV (ME AoV SAX, ME AoV LAX views), and coronary artery dilation and coronary ostial obstruction (ME AoV SAX, ME AoV LAX views). Evaluation for possible coronary ostial obstruction is best performed with color mapping, looking for turbulence in the area of stenosis [66–68]. The TG Mid Pap SAX and TG Basal SAX views can also be used to evaluate for segmental wall motion abnormalities, supporting the possibility of coronary artery obstruction. The branch pulmonary arteries should also be evaluated for possible stenosis using the midesophageal ascending aorta short axis (ME Asc Ao SAX), upper esophageal pulmonary artery (UE PA), and UE

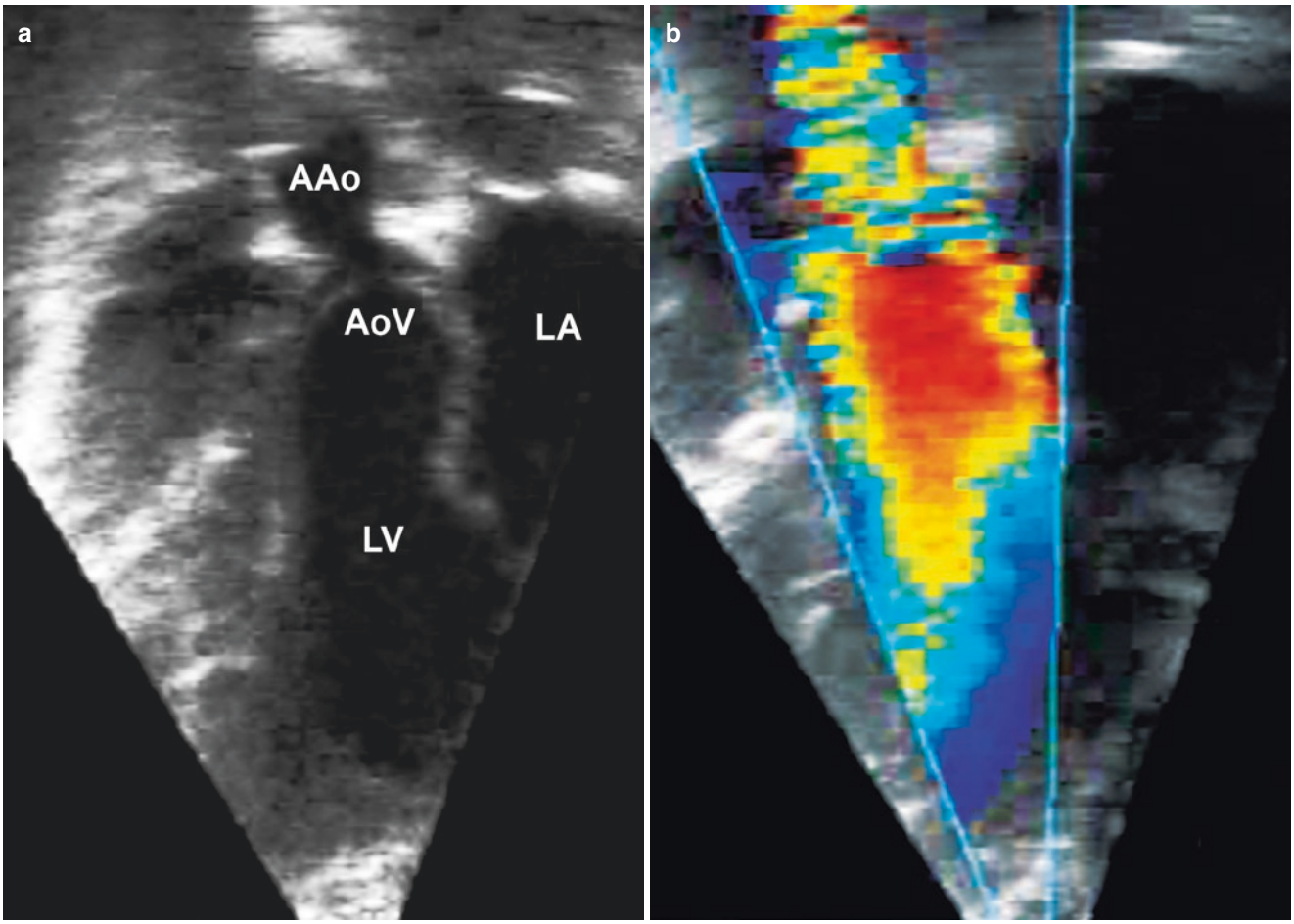

Fig. 13.13 Deep transgastric five-chamber view at 30° showing discrete narrowing of the sinotubular junction resulting in supravalvar aortic stenosis (**a**) two-dimensional imaging and (**b**) color flow mapping (*AAo* ascending aorta, *AoV* aortic valve, *LA* left atrium, *LV* left ventricle)

Ao Arch SAX views. The branch pulmonary arteries can be difficult to evaluate by TEE, although color mapping can be quite helpful in ascertaining the presence and location of branch pulmonary artery stenosis (Chaps. 4 and 16).

Postoperative residual supravalvar aortic obstruction should be excluded by TEE qualitatively in the ME AoV LAX and ME Asc Ao LAX views (transducer angle for both at ~120°), and quantitatively in the DTG 5-Ch, DTG RVOT, and TG LAX views. The AoV leaflets should be re-evaluated in the ME AoV SAX view at 30° to 45°. Using the multiple midesophageal and deep transgastric views mentioned above, a thorough search should be performed for other possible levels of stenosis that could have been masked in the presence of distal obstruction.

Aortic Regurgitation

Isolated congenital AR, defined loosely as diastolic flow from the aortic root into the LV, is a rare lesion [69]. Congenital etiologies causing AR in childhood include a bicuspid or quadricuspid AoV, (Fig. 13.14, Video 13.14) a dysplastic tricuspid AoV, an aortico-LV tunnel, absence of one or more AoV leaflets, a coronary-cameral fistula into the LV, and a ruptured sinus of Valsalva aneurysm into the LV. Occasionally AR occurs in the setting of subvalvar AS (as discussed previously), AoV prolapse into a perimembranous VSD or a doubly-committed subarterial VSD, a ruptured sinus of Valsalva aneurysm into the right atrium (Fig. 13.15, Videos 13.15a and 13.15b) . It can also be seen with aortic root dilation in neonatal Marfan syndrome, tetralogy of Fallot, or truncus arteriosus. Acquired AR generally occurs with endocarditis, rheumatic fever, or after surgical or transcatheter balloon valvotomy for valvar AS. In general, AR is a progressive disease. The increased volume load on the LV initially results in compensatory hypertrophy, although the degree of hypertrophy becomes inadequate as regurgitation worsens (decompensated AR). Increasing LV volume associated with decreasing ventricular wall thickness results in increased afterload, and eventually there is myocardial damage and diminished contractility secondary to the increased afterload. In an effort to prevent irreversible myocardial damage, some echocardiographic guidelines have been established regarding the

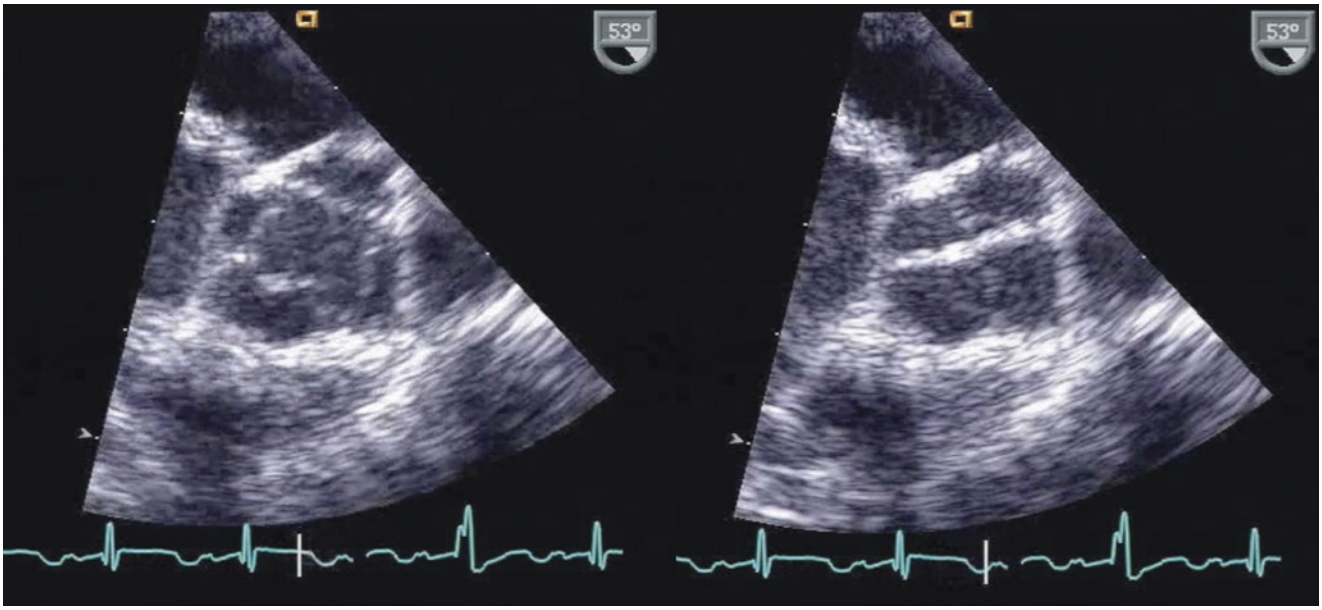

Fig. 13.14 Quadricuspid aortic valve as seen from the midesophageal aortic valve short axis view, in systole (left figure) and diastole (right figure)

timing for intervention. In 2014, the American College of Cardiology and American Heart Association Task Force on Practice Guidelines recommended an end-diastolic diameter of 65 mm and an end-systolic diameter of 55 mm (as measured in transthoracic parasternal short axis views of the LV) as thresholds for intervention in asymptomatic adults with significant AR [22]. Comparable guidelines for the pediatric population have not yet been established.

The utility of transthoracic echocardiography in assessing the degree of AR and the appropriate timing for intervention has been discussed extensively [70]. Once a patient is in the operating room, the goals of the preoperative TEE are to assess: a) the mechanism for AR, b) the degree of aortic regurgitation, and c) LV size and function. Whether the AR is secondary to annular dilation, cusp prolapse (in the setting of a VSD), or cusp deficiency as in a bicuspid AoV or in rheumatic heart disease [71] is especially important if surgical repair of the valve is a consideration, as valves with bicuspid morphology and those after rheumatic fever tend to be better candidates for surgical repair [72] . TEE should evaluate the AoV and aortic root morphology in multiple midesophageal views, including the ME 5-Ch view at 0°–10°, and the ME LAX and ME AoV LAX at 120°–140°. The ME AoV SAX view at 30°–45° will display abnormalities in AoV commissural morphology, discrepancies among the individual leaflet sizes, absence of one or more of the leaflets, dilation of a coronary artery in the setting of a significant coronary-cameral fistula into the LV, disruption of one or more AoV leaflets (flail segment) secondary to endocarditis or after valvotomy, or rupture of a sinus of Valsalva into one of the intracardiac chambers (Fig. 13.15a, Video 13.15a). The ME AoV LAX view at ~120° and ME RV In-Out view between 60°–90° will also display a ruptured sinus of Valsalva aneurysm (Fig. 13.15b, Video 13.15b). These orthogonal views will also be useful for evaluating other causes of AR, such as an abnormally thickened AoV leaflets after rheumatic fever, or an aortico-LV tunnel (Fig. 13.16, Video 13.16). The location of the regurgitant jet should be assessed from multiple TEE windows, including the midesophageal (ME AoV SAX, ME AoV LAX, ME LAX), deep transgastric (DTG 5-Ch, DTG RVOT), and transgastric (TG LAX) views. Narrow angle 3D TEE imaging with adequate frame rate and color mapping can help in the assessment of the mechanism and degree of regurgitation. Biplane two-dimensional imaging allows two views to be obtained at the same time and can thus save time.

When assessing the severity of AR, a 2017 report from the American Society of Echocardiography Task Force on Valvular Regurgitation suggests that a vena contracta width for the regurgitant jet >0.6 cm and a ratio between the vena contracta width and the LV outflow tract diameter > 65% represent severe AR [72]. Both of these measurements are best obtained from the ME AoV LAX view. In keeping with these recommendations, the 2014 ACC/AHA guidelines and the 2017 American Society of Echocardiography guidelines [72] listed the following echocardiographic criteria for classification of AR:

- Mild: Vena contracta width < 0.3 cm, jet width/LVOT diameter < 25%
- Moderate: Vena contracta width 0.3–0.6 cm, jet width/LVOT diameter 25–65%
- Severe: Vena contracta width > 0.6 cm, jet width/LVOT diameter > 65%

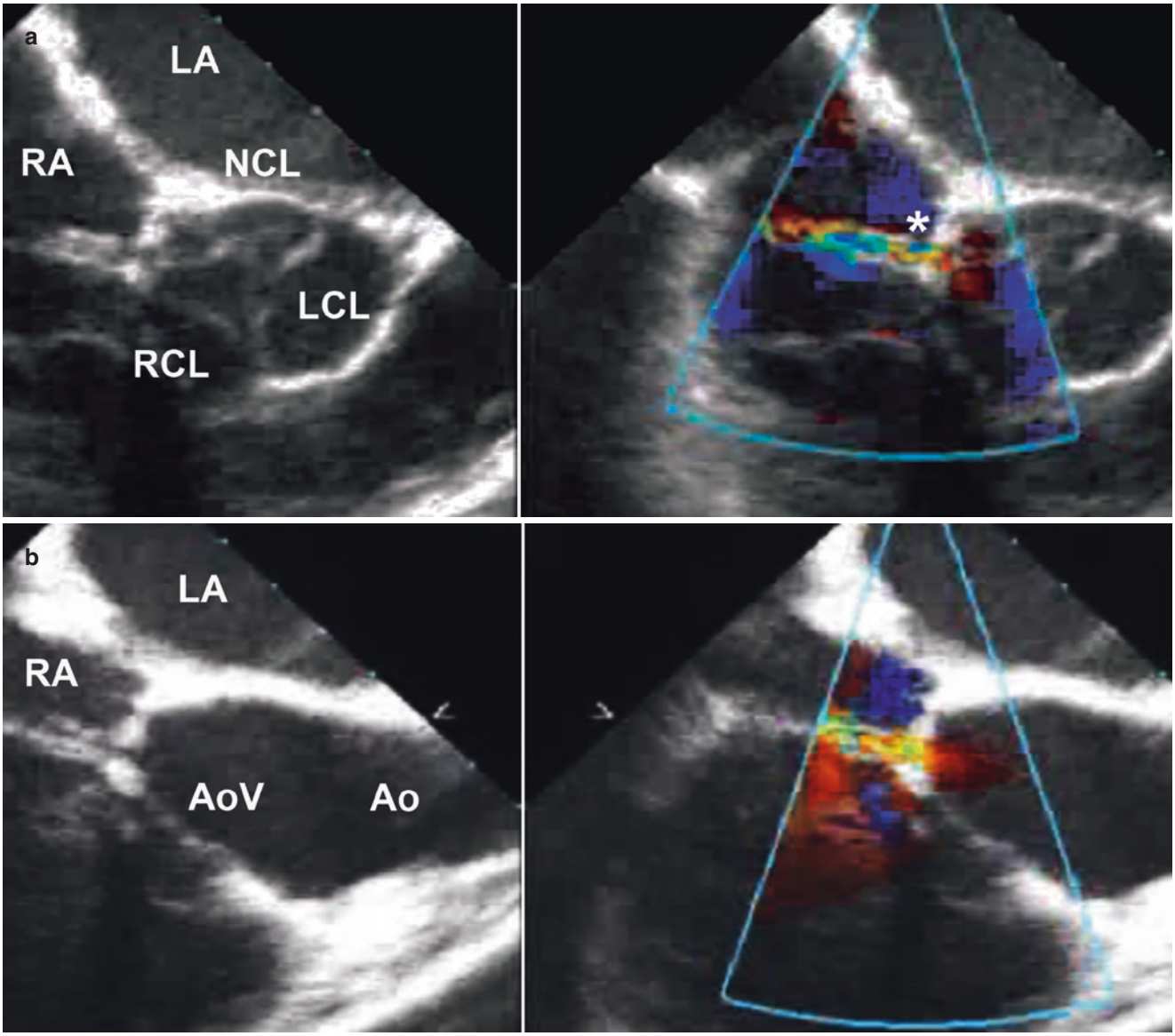

Fig. 13.15 (**a**) Midesophageal aortic valve short axis view at 45° displaying an *en face* view of the aortic valve and a ruptured non-coronary sinus of Valsalva aneurysm (asterisk) into the right atrium; (**b**) Modified midesophageal right ventricular inflow-outflow view at 90° showing the same ruptured of sinus of Valsalva aneurysm into the right atrium (*Ao* aorta, *AoV* aortic valve, *LA* left atrium, *LCL* left coronary leaflet, *NCL* non-coronary leaflet, *RA* right atrium, *RCL* right coronary leaflet)

Other supportive data that can indicate at least moderate AR include prominent retrograde diastolic flow in the descending aorta, as noted by both color mapping and pulsed wave Doppler interrogation [20, 21, 73]. This can best be evaluated using a combination of upper esophageal (UE Ao Arch LAX, SAX) and descending aorta long axis (Desc Ao LAX) and descending aortic short axis (Desc Ao SAX) views. There are few data on the utility of TEE to evaluate other indices of AR severity such as pressure half-time (which reflects the rate of equalization of aortic and LV diastolic pressures in the setting of AR), especially since this index can be affected by LV compliance, LV diastolic pressures, aortic compliance, and any therapy which changes ventricular afterload [73, 74]. In general, a pressure half-time > 500 ms is usually compatible with mild AR, while a value < 200 ms is consistent with severe AR [72]. Methods that have been discussed in other sources, but are rather difficult and time-consuming to perform in the intraoperative setting, include the calculation of effective regurgitant orifice area (EROA) by the flow convergence method (proximal isovelocity surface area or PISA) [72, 75]. If used, the following grading system (EROA in cm^2) has been suggested: mild AR <0.10, moderate AR 0.10–0.30 severe AR > 0.30 [22]. It should be noted that the degree of AR can be difficult to assess by TEE, particularly in the

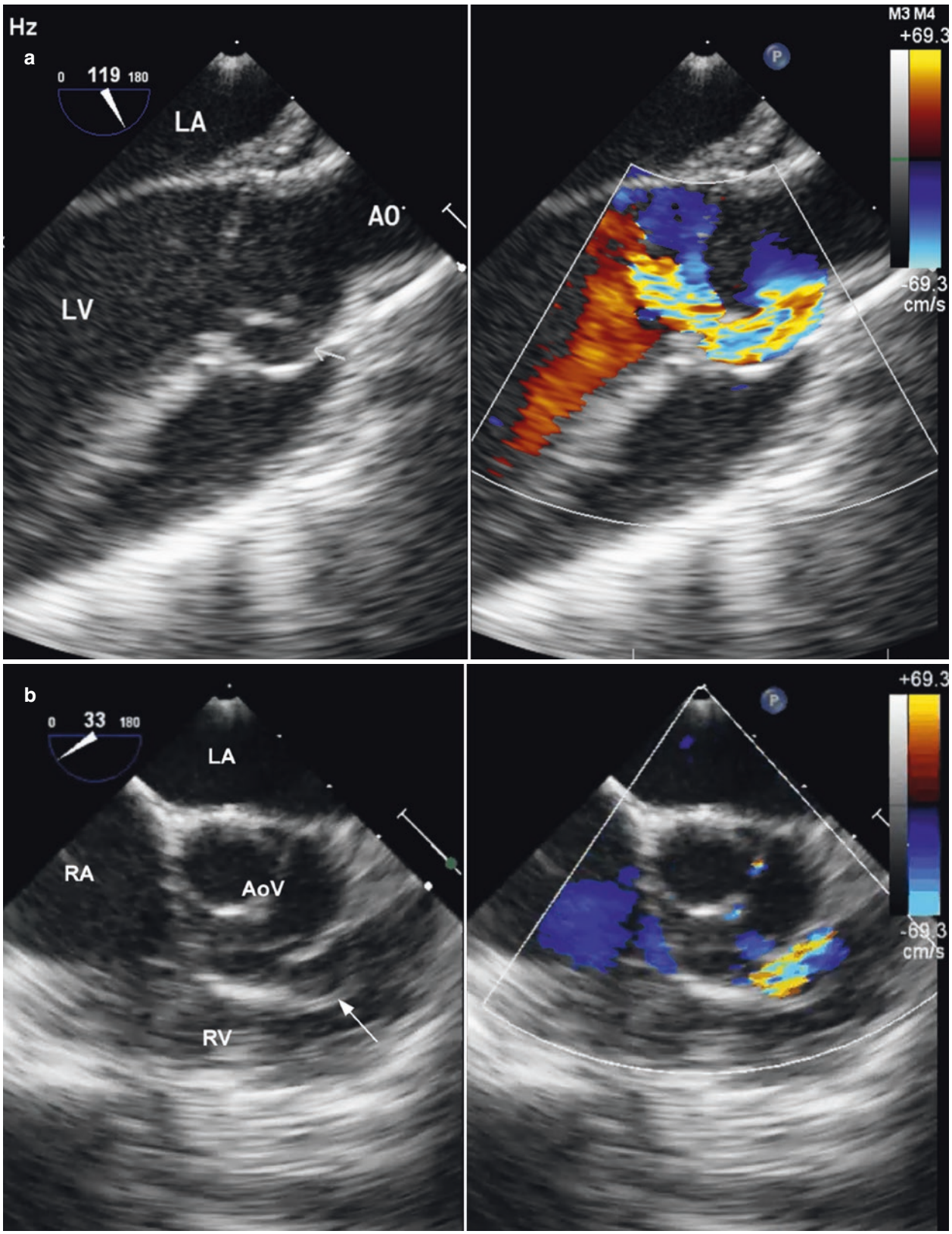

Fig. 13.16 Aortico-left ventricular tunnel. (**a**) Shows a midesophageal aortic valve long axis view, with the aortico-left ventricular tunnel (arrow) anterior to the right coronary cusp. There is significant regurgitation from the aorta (AO) to the left ventricle (LV) through this tunnel in diastole. (**b**) Taken from a midesophageal aortic valve short axis view, this image shows the aortic valve (AoV) *en face* as well as the tunnel (arrow) anterior to the right coronary cusp. (*LA*, left atrium, *RA*, right atrium, *RV*, right ventricle)

operating room in which changing hemodynamics and general anesthesia could artificially alter its severity. However, in a cohort of pediatric patients who had undergone aortic valve repair, Honjo et al. found that, using the jet width/LVOT criteria, there was reasonable agreement between the degree of AR found by intraoperative TEE and subsequently by predischarge transthoracic echocardiogram [76]. In addition to the evaluation of AR, LV size and function should be assessed qualitatively in the transgastric short axis views (TG Mid Pap SAX, TG Basal SAX) at 0°. Associated abnormalities such as subvalvar AS, a VSD, and aortic dilation can be assessed in multiple views as discussed above.

Surgical intervention generally involves aortic valvuloplasty (occasionally involving the use of autologous pericardium), Ozaki procedure, a Ross procedure (involving replacement of the aortic root with the patient's pulmonary root and placement of a homograft from the RV to the pulmonary artery), or AoV replacement with a mechanical valve, bioprosthesis, or homograft valve. The postoperative TEE should exclude residual LVOT obstruction using the transgastric LAX and deep transgastric views: DTG 5-Ch at 0 – 30°, and DTG RVOT view at ~90°. Residual AR can be evaluated in multiple midesophageal, transgastric, and deep transgastric views. After aortic valvuloplasty, a systolic maximum instantaneous gradient > 45 mmHg and degree of AR ≥ moderate are considered indications to return to cardiopulmonary bypass for a repeat AoV repair or replacement [77]. Coaptation asymmetry after AoV repair assessed from a short axis view of the AoV on postoperative TEE is a predictor of early reoperation for residual AR after AoV surgical repair [78]. After a Ross procedure, any neo-AR is a highly sensitive predictor of ≥ moderate neo-AR at the time of hospital discharge [79]. If a prosthetic AoV is present, symmetric motion of the valve leaflets can usually be seen in the midesophageal views, particularly the ME AoV SAX and ME AoV LAX views (Fig. 13.17, Video 13.17), though this can become difficult secondary to acoustic interference from the prosthetic valve annular ring. The transgastric and deep transgastric views are helpful here: because they visualize the valve from the LV aspect, they avoid shadowing and reverberation artifacts, allowing evaluation of the "upstream" portion of the prosthetic valve and leaflet motion. Doppler evaluation of the prosthetic valve should be performed from the transgastric or deep transgastric views, as described above and discussed in Chap. 19.

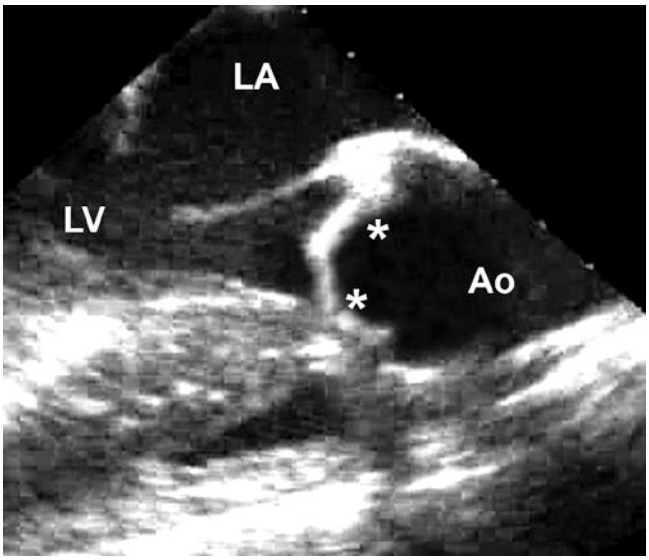

Fig. 13.17 Midesophageal aortic valve long axis view at 120° showing a prosthetic aortic valve with symmetric positioning of the prosthetic hemidisc leaflets (asterisks) (*Ao* aorta, *LA* left atrium, *LV* left ventricle)

Aneurysm of the Proximal Aorta

Formation of an aortic root aneurysm and aneurysmal dilation of the proximal aorta result from an intrinsic aortopathy, usually involving smooth muscle cell loss and extracellular matrix disruption (cystic medial necrosis). These structural abnormalities in the muscular and elastic components lead to thinned and weakened aortic walls. As seen in supravalvar AS, abnormalities in elastin homeostasis may play a major role in the development of aortic root aneurysms and a dilated proximal aorta. For example, Marfan syndrome, with its predilection for aortic root dilation, is caused by mutations in the fibrillin gene on chromosome 15 [80], and fibrillin is an important glycoprotein necessary for elastin production and maintenance [81]. Associations with dilation of the proximal aorta include Marfan syndrome, Loeys-Dietz syndrome, Ehlers-Danlos syndrome, Turner syndrome, a bicuspid AoV, systemic hypertension, and aortic coarctation. Congenital cardiac defects known to be associated include tetralogy of Fallot, transposition of the great arteries, and truncus arteriosus [82]. Because of the intrinsic weakness in the aortic wall, a sinus of Valsalva aneurysm is at risk for rupture into the right and left heart chambers (most frequently into the RV) [83] (Fig. 13.15, Videos 13.15a and 13.15b), and a dilated aortic root (Fig. 13.18, Video 13.18) or ascending aorta is at risk for dissection and rupture [84] (Fig. 13.19, Video 13.19). Both of these problems are frequently associated with AR [85, 86]. In addition, aortic root aneurysms can be associated with a VSD [83]. Generally, these patients undergo cross-sectional imaging using computed tomography (CT) or magnetic resonance inaging (MRI) in order to evaluate completely the aortic valve, aortic root, and ascending/descending aorta. TEE is frequently superior to transthoracic echocardiography in the evaluation of the entire extent of the proximal aorta, particularly in older children and in adults, and occasionally a TEE study is performed before the decision to intervene surgically is made. Midesophageal views at multiple angles can display a sinus of Valsalva aneurysm as well as its spatial relationship to surrounding cardiac structures. Color

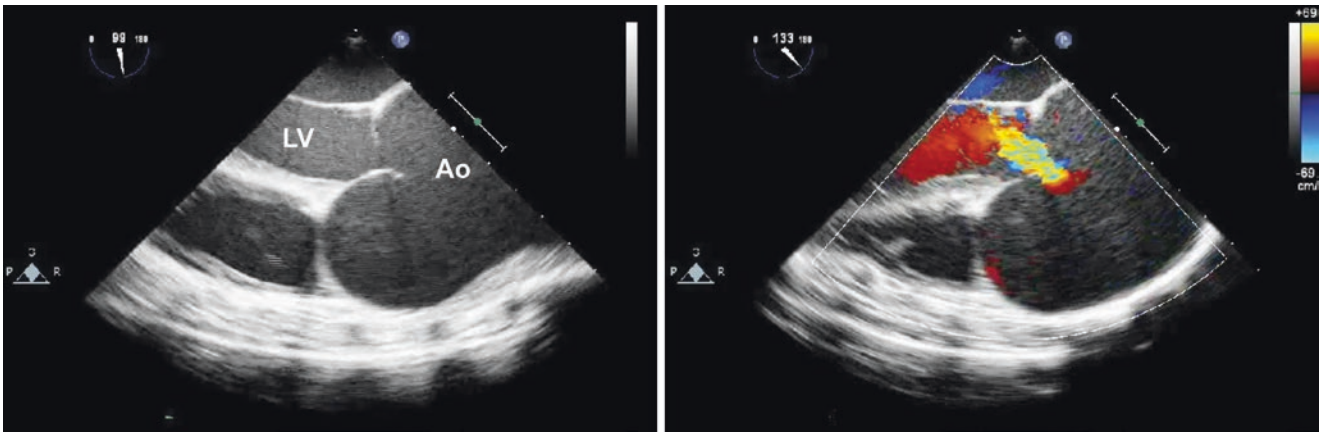

Fig. 13.18 Markedly dilated aortic root as seen from the midesophageal aortic valve long axis view without color mapping (left panel) and with color mapping, showing central aortic regurgitation (right panel). (*Ao* aorta, *LV* left ventricle)

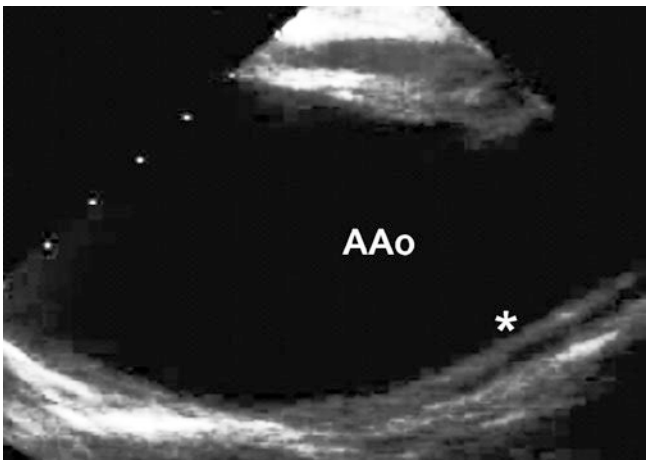

Fig. 13.19 Midesophageal ascending aortic long axis view at 120° showing a markedly dilated aortic root and ascending aorta with associated aortic dissection along the anterior wall of the ascending aorta (the double linear density representing the aortic dissection along the anterior ascending aortic wall is indicated by the asterisk) in a patient with Marfan syndrome (*AAo* ascending aorta)

mapping can easily display the continuous restrictive jet of a ruptured aneurysm into the right atrium, RV, and left atrium; when the aneurysm ruptures into the LV, color mapping can display the diastolic jet. The location and degree of AR can also be evaluated with color mapping in multiple midesophageal views. Aneurysmal dilation of the aortic root and ascending aorta is best evaluated with ME Asc Ao LAX view between 90° to 130° (Fig. 13.18, Video 13.18). One should always look for the characteristic parallel lines of dissection along the aortic wall in these patients from multiple midesophageal views (Fig. 13.19, Video 13.19), and color mapping will occasionally show the connection between the dissection and the aortic lumen. The more superior portion of the ascending aorta, as well as aortic arch and proximal descending aorta, can also be evaluated for dilation and possible dissection using the upper esophageal TEE views (UE Ao Arch SAX at 70°–90°, UE Ao Arch LAX at 0°). See Chap. 20 for further discussion on the TEE evaluation of aortic dissection.

Right Ventricular Outflow Tract Anomalies

Valvar Pulmonary Stenosis

Valvar PS is one of the most commonly occurring types of CHD [1, 2]. It can present either as thin but doming leaflets with tricuspid or bicuspid morphology or as dysplastic leaflets with thickened edges. The former represents the more common presentation and is often associated with post-stenotic dilation of the main pulmonary trunk (Fig. 13.20, Video 13.20). Because one or more of the commissures can be partially or completely fused or underdeveloped (with formation of a raphe), the thickened raphe can appear tethered to the arterial wall at the sinotubular junction, giving the lesion the appearance of supravalvar narrowing (Fig. 13.20, Video 13.20). As discussed previously, the semilunar valve attachments extend up to the sinotubular junction [86] (Fig. 13.3b), and this particular variant of valvar PS can sometimes be difficult to distinguish from discrete narrowing of the pulmonary sinotubular junction (supravalvar stenosis) without valvar obstruction. Because of the underdeveloped distal segments of the commissures, the leaflets are often attached in a more circular fashion at the pulmonary root rather than the normal semilunar arrangement discussed previously [87]. The dysplastic form of valvar PS is not as common and is often associated with pulmonary annular hypoplasia and a small pulmonary trunk. The leaflets are usually attached to the pulmonary root in a semilunar fashion. Occasionally there is separate but discrete narrowing of the pulmonary sinotubular junction resulting in combined valvar and supravalvar PS. Valvar PS places excess pressure load on the RV,

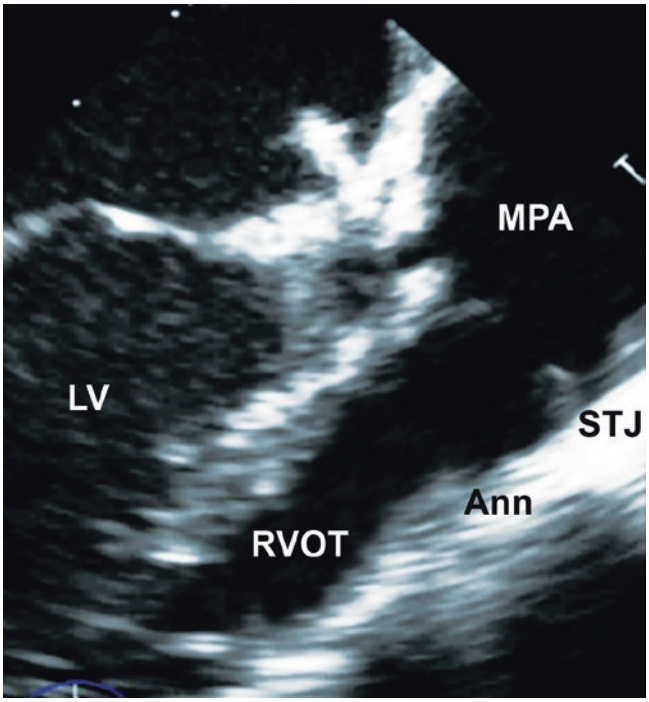

Fig. 13.20 Midesophageal aortic valve long axis view with transducer angle at 90° and slight leftward probe rotation. This image shows valvar pulmonary stenosis with thin but doming pulmonary valve leaflets abutting against the sinotubular junction and post stenotic dilation of the main pulmonary artery (*Ann* pulmonary annulus, *LV* left ventricle, *MPA* main pulmonary artery, *RVOT* right ventricular outflow tract, *STJ* pulmonary sinotubular junction)

often resulting in significant RV hypertrophy, which in turn can contribute to the total obstruction along the RVOT. An atrial septal defect or patent foramen ovale is also commonly found in these patients [88].

Because the majority of these patients undergo intervention when necessary in the catheterization laboratory, TEE is rarely needed to evaluate the PV morphology and degree of obstruction. However, TEE is frequently used during transcatheter device closure of atrial septal defects, and the excess pulmonary blood flow associated with these lesions often results in turbulence across the PV without true valvar PS (relative PS). TEE performed in the catheterization laboratory can help determine whether intervention is necessary at the PV. The RVOT, and particularly the PV, can easily be evaluated in ME AoV SAX at 0° and a modified ME AoV LAX at 90° with leftward probe rotation to visualize the pulmonary outflow tract (Fig. 13.20, Video 13.20). Occasionally, a higher esophageal view, such as ME Asc Ao SAX or upper esophageal view (UE PA at 0°, UE Ao Arch SAX at 90°), is necessary in patients with an elongated subpulmonary conus. Quantitative assessment of the degree of valvar PS can be performed from the DTG RVOT view at 90° (Fig. 13.1b, d; Video 13.1b) in the same way that LVOT obstruction is evaluated by Doppler interrogation, usually requiring a counterclockwise rotation of the probe (to the left) from the LVOT to the RVOT. The degree of valvar PS can also be assessed in the ME Asc Ao SAX or UE PA view at 0° by interrogating the high velocity flow into the main pulmonary trunk (Figs. 13.21 and 13.22, Video 13.21). This view also allows for measurements of the main and proximal branch pulmonary artery diameters. In many instances, these views or the UE Ao Arch SAX provides an excellent angle for Doppler interrogation of the high velocity jet arising from the PV. (Video 13.20)

There are a number of congenital heart defects in which pulmonary stenosis (subvalvar, valvar, and sometimes supravalvar) is a frequent finding. At times, pulmonary outflow obstruction is an important and integral part of the anatomic spectrum of the cardiac defect. Examples of such anomalies include tetralogy of Fallot, double outlet right ventricle, tricuspid atresia, and transposition of the great arteries, and these cardiac defects are discussed in other chapters in this textbook. Nonetheless, the TEE evaluation of the pulmonary outflow tract in those conditions mirrors that described in this chapter, and should be performed using a similar approach.

Subvalvar Pulmonary Stenosis (Double Chamber Right Ventricle)

A double chamber right ventricle (DCRV) is a type of RVOT obstruction involving anomalously prominent RV muscle bundles that divide the RV into two chambers: a proximal high-pressure inflow chamber and a distal low-pressure outflow chamber (Figs. 13.23 and 13.24, Videos 13.22 and 13.23). Some prefer to use the term divided RV for this lesion [89], although a divided RV does not always involve anomalous RV muscle bundles [90]. The division in a DCRV usually occurs at the infundibular os, with the distal outflow chamber corresponding to a well-developed subpulmonary infundibulum. Like subvalvar AS, the obstruction associated with a DCRV is not always present early in life, prompting some people to classify the lesion as an acquired disease [91]. However, others suggest that a congenital anatomic substrate for a DCRV is present before obstruction develops and can actually be predicted echocardiographically by measuring the distance from the moderator band to the PV [92]. In this setting, a DCRV is thought to result from superior displacement and hypertrophy of the moderator band, contributing to progressive obstruction at the infundibular os. Others suggest,

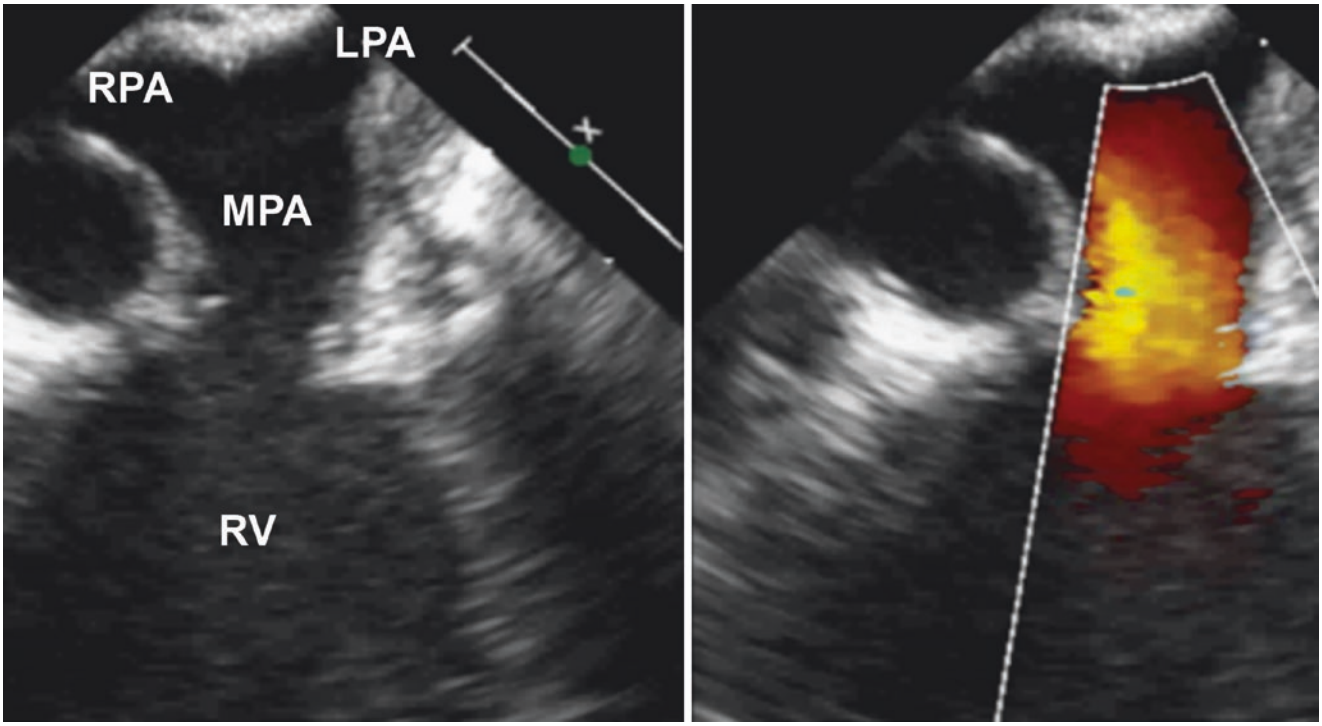

Fig. 13.21 Upper esophageal pulmonary artery view at 0° showing the main pulmonary artery in the setting of mild valvar pulmonary stenosis with thin doming pulmonary valve leaflets, and minimal flow acceleration across the valve. In this image the bifurcation of the branch pulmonary arteries can also be seen (*LPA* left pulmonary artery, *MPA* main pulmonary artery, *RPA* right pulmonary artery, *RV* right ventricle)

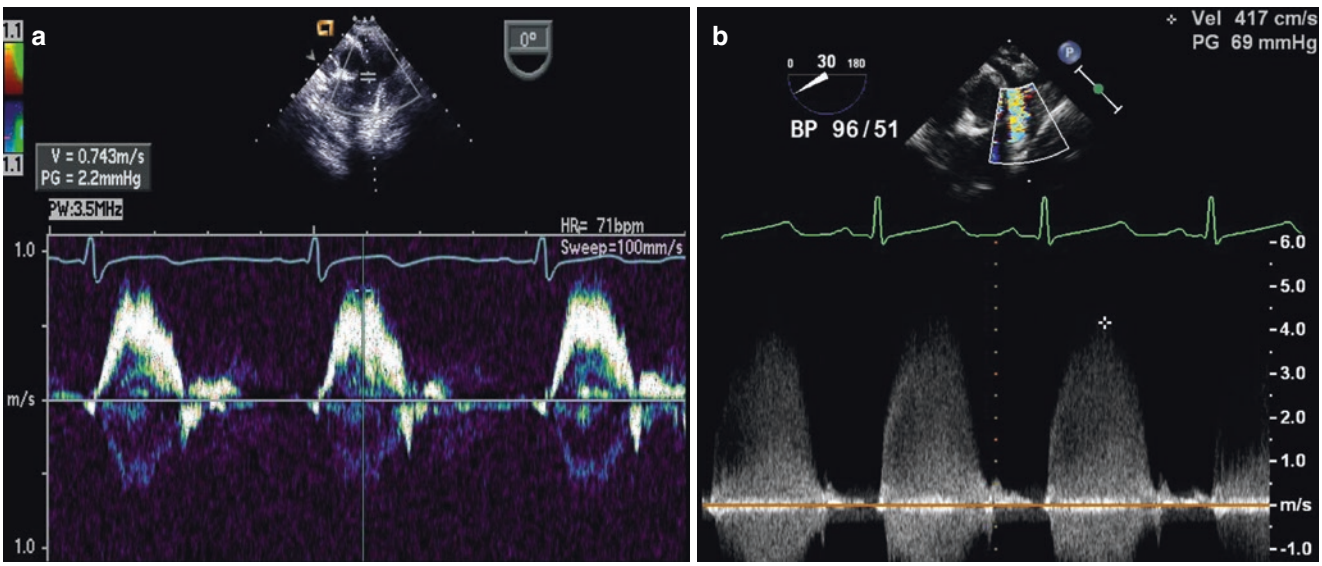

Fig. 13.22 Spectral Doppler recordings of flow across the pulmonary valve, as obtained from the upper esophageal pulmonary artery view at 0°. In: (**a**), there is normal, low velocity laminar flow seen in the main pulmonary artery through a normal pulmonary valve. (**b**), high velocity flow (4.2 meters/sec, 69 mm Hg) is obtained by continuous wave Doppler across a pulmonary valve that is stenotic

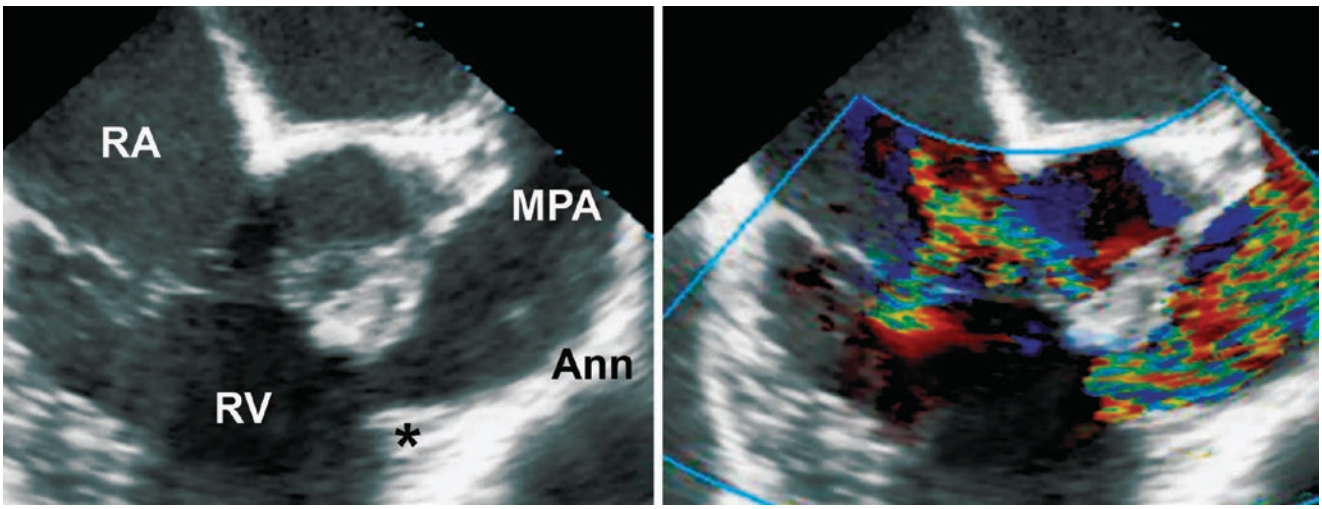

Fig. 13.23 Midesophageal right ventricular inflow-outflow view at 60° showing a double chamber right ventricle with prominent muscle bundles at the infundibular os (*asterisk*) separating the proximal right ventricular chamber from the well-developed right ventricular infundibular chamber and resulting in subvalvar pulmonary stenosis (the pulmonary annulus is within normal limits in size). Moderate tricuspid regurgitation is also present. (*Ann* pulmonary annulus, *MPA* main pulmonary artery, *RA* right atrium, *RV* right ventricle)

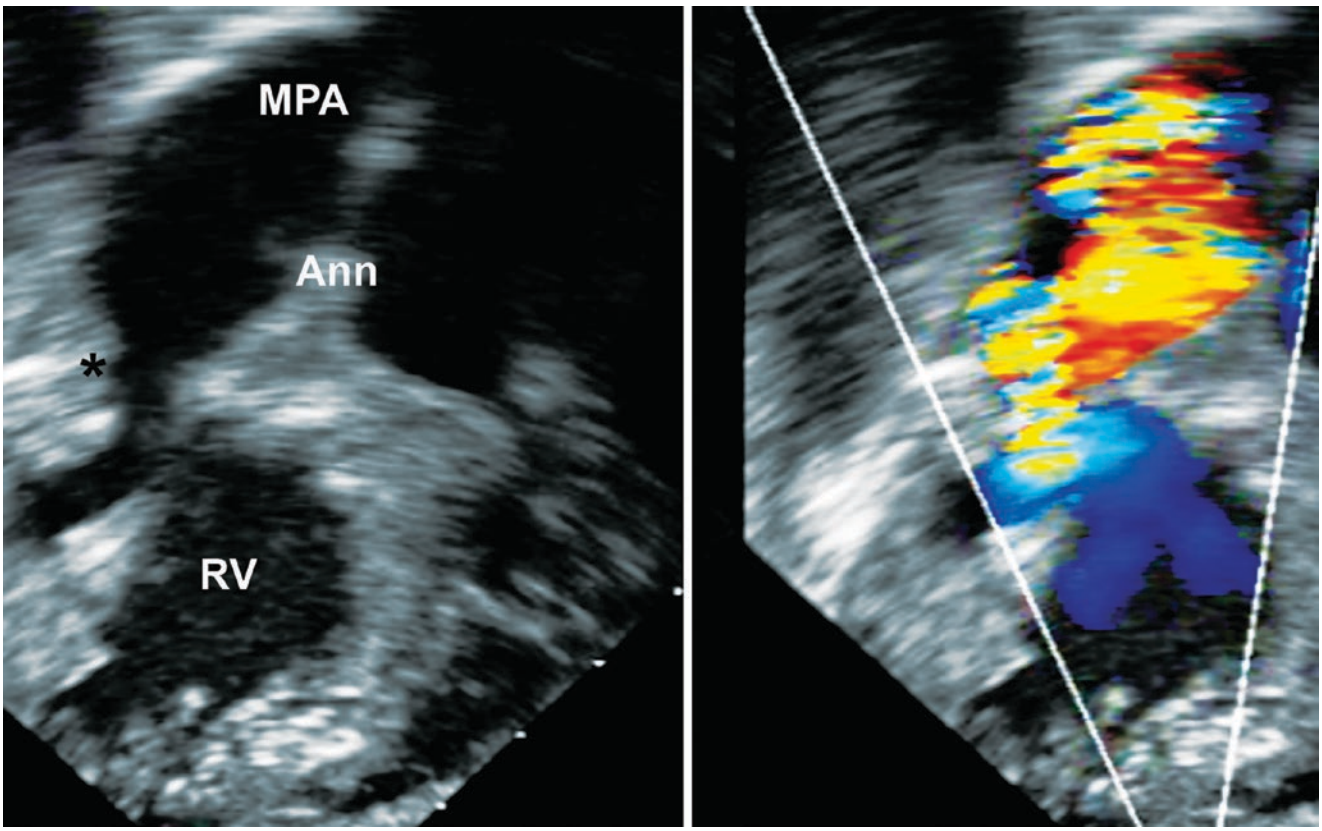

Fig. 13.24 Deep transgastric right ventricular outflow tract view at 90° showing a double chamber right ventricle with prominent muscle bundles at the infundibular os (asterisk) separating the proximal right ventricular chamber from the well-developed right ventricular infundibular chamber and resulting in subvalvar pulmonary stenosis (the pulmonary annulus is within normal limits in size); this is an ideal view to measure the gradient along the right ventricular outflow tract. (*Ann* pulmonary annulus, *MPA* main pulmonary artery, *RV* right ventricle)

however, that the anomalously prominent muscle bundles in a DCRV are in fact distinct from the moderator band since the septal attachment of a normal moderator band is located more apically than the usual attachments of these anomalous muscle bundles [93]. The most common association is a VSD, usually a small or moderate perimembranous VSD, occurring in at least 67% of these patients [94]. It can be present in up to 10% of patients who require VSD surgery [95], necessitating careful assessment of the RVOT in all patients with a VSD. Another common association is a fixed subaortic ridge or echodense area at the crest of the ventricular septum, occurring in up to 88% of patients with a DCRV and a VSD, although some degree of subvalvar AS is present in only a quarter of these patients [53]. A DCRV must be distinguished from tetralogy of Fallot, wherein anterior and superior deviation of the conal septum results in a large VSD and an underdeveloped subpulmonary infundibulum.

The RVOT obstruction in DCRV is usually progressive, presenting during childhood or adolescence, although cases of adult presentation have been reported [94, 96]. Almost all cases require surgical intervention. TEE is useful in the preoperative evaluation, and the infundibular os and RVOT are easily visualized in the ME RV In-Out view with transducer angle between 60°–90°. However, the anterior location of the prominent muscle bundles and their proximity to the probe often makes qualitative assessment of the extent of the muscle bundles difficult. Thus, this area should be examined carefully as it is easy to overlook RVOT obstruction at this level. In addition, the orientation of blood flow across the muscle bundles is often directly perpendicular to the echocardiographic beam in midesophageal views, precluding adequate color mapping and quantitative spectral Doppler interrogation of the area (Fig. 13.23, Video 13.22). Quantitative assessment of the degree of RVOT obstruction is best performed in the DTG RVOT view at 90° as discussed in the previous section (Fig. 13.24, Video 13.23). Postoperative evaluation after resection of the muscle bundles should exclude residual obstruction in the DTG RVOT view at 90°; the TEE study should evaluate for the development of pulmonary regurgitation in multiple midesophageal views. Occasionally, resection of the muscle bundles results in the development of tiny coronary-cameral fistulae along the RV anterior free wall, and these are easily visualized with color mapping in multiple midesophageal views.

Pulmonary Regurgitation

Pulmonary regurgitation (PR) is a common finding during routine echocardiographic evaluation with a prevalence of up to 88% in normal healthy children and up to 68% in healthy adults [97]. The prevalence may decrease later in adulthood, although this trend may be more related to technical limitations in adults with poor echocardiographic windows rather than a true decrease in the frequency of the lesion. Among the 3370 subjects with pulmonary outflow tract anomalies evaluated by echocardiography at Children's Hospital Boston from 1988 to 2002, over 40% (1403) had PR and almost 24% of these (335) had ≤ mild PR without associated cardiac structural abnormalities [98]. Isolated PR as a congenital anomaly is extremely rare and has been associated with aneurysmal dilation of the pulmonary arteries secondary to cystic medial necrosis (as seen in the aortopathy of Marfan syndrome and bicuspid AoV) [99]. Many of these patients do not require intervention, unless the severity of the PR results in significant RV dilation and dysfunction. Occasionally, isolated PR with idiopathic dilation of the pulmonary arteries is associated with absence of one or more PV leaflets [99, 100]. Although this is seen more frequently in the setting of tetralogy of Fallot with absent or dysplastic PV leaflets, it can occur as an isolated abnormality, and marked dilation of the pulmonary arteries can also occur, resulting in significant airway compression that requires surgical intervention.

Quantification of PR is not as well established by echocardiography (either transthoracic or transesophageal). Doppler methods, both color flow and spectral, are generally used, though variable hemodynamic conditions (RV diastolic properties and filling pressures, driving pressure between pulmonary artery and RV, etc.) will influence the Doppler evaluation. Pulsed wave Doppler assessment of the forward and reverse flow in the main pulmonary artery (using the velocity time integral) could theoretically be used to estimate the percent and volume of regurgitant flow; however, this method has not been standardized and also is not valid in patients with valvar PS. Criteria for vena contracta width (which would seem to be more accurate than jet width) and regurgitant orifice area width to assess PR severity have not been well established [73]. Indirect evidence of PR severity can be obtained by evaluating RV size and function, though this can be more challenging by echocardiography due to the more complex shape of the RV. Also, the RV diastolic properties (specifically the stiffness) can affect the degree of RV dilation. Some of the features commonly used to grade PR severity are listed in Table 13.1 [72]. Overall, it is clear that the grading of PR severity is more difficult because standards for its quantification are less well defined than for AR [72, 101]. Thus, when assessing severity of PR, an integrated approach is probably best, utilizing color mapping, continuous and pulsed wave Doppler interrogation, as well as evaluations of the PV and RV sizes and RV function [76].

The most common scenarios for significant PR occur after some type of intervention: after surgical repair of tetralogy of Fallot (Fig. 13.25, Video 13.24), after surgical or transcatheter balloon valvotomy for valvar PS, and after surgical placement of a homograft from the RV to the pul-

Table 13.1 Echocardiographic and Doppler parameters used in grading pulmonary regurgitation severity

Parameter	Mild	Moderate	Severe
Pulmonic valve	Normal	Normal or abnormal	Abnormal or may not be visible
RV size	Normal[a]	Normal or dilated	Dilated (exception: Acute PR)
Jet size by color flow Doppler[b]	Thin (usually <10 mm in length) with a narrow origin	Intermediate	Broad origin, variable depth of penetration
Ratio of PR jet width/pulmonary annulus			>0.7 (identifies a CMR-derived PR fraction ≥40%)
Jet density and contour—CW	Soft	Dense	Dense; early termination of diastolic flow
Deceleration time of the PR spectral Doppler signal[c]			Short, < 260 msec
Pressure half-time of PR jet			<100 msec[d]
PR index[e]		<0.77	>0.77
Diastolic flow reversal in the main or branch PAs (PW)			Prominent
Pulmonic systolic flow compared to systemic flow—PW[f]	Slightly increased	Intermediate	Greatly increased
RF[g]	<20%	20%–40%	>40%

CMR cardiac magnetic resonance, *CW* continuous wave Doppler, *PR* pulmonary regurgitation, *PW* pulsed wave Doppler, *RA* right atrium, *RF* regurgitant fraction, *RV* right ventricle

[a]Unless there are other reasons for RV enlargement

[b]At a Nyquist limit of 50–70 cm/s

[c]Steep deceleration is not specific for severe PR

[d]Not reliable in the presence of high RV end diastolic pressure

[e]Defined as the duration of the PR signal divided by the total duration of diastole, with this cutoff identifying a CMR-derived PR fraction >25%

[f]Cut-off values for regurgitant volume and fraction are not well-validated

[g]Regurgitant fraction data primarily derived from CMR with limited application by echocardiography

Table reprinted from Zoghbi WA et al (72) with permission from Elsevier

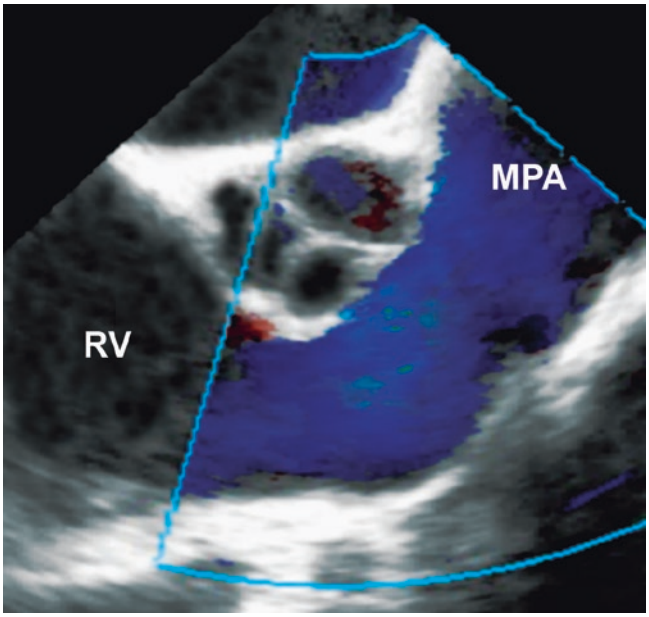

Fig. 13.25 Midesophageal right ventricular inflow-outflow view at 60° showing free pulmonary regurgitation in the setting of tetralogy of Fallot repair with a transannular right ventricular outflow tract patch. (*MPA* main pulmonary artery, *RV* right ventricle)

monary artery for lesions such as tetralogy of Fallot (with or without pulmonary atresia), truncus arteriosus, transposition of the great arteries with a VSD, and pulmonary atresia with intact ventricular septum. As in patients with significant AR, significant PR is associated initially with an increase in RV end-diastolic volume, followed by an increase in RV end-systolic volume, followed by a decrease in RV function and contractility. Symptoms of right-sided heart failure appear, portending the development of irreversible RV myocardial damage. In many postoperative instances, there are markedly akinetic segments of the RV due to outflow tract patch augmentation and aggressive muscular resection, contributing to the progressive RV systolic and diastolic dysfunction. In addition, newly acquired, significant postoperative PR is not well tolerated by older patients, unlike neonates and children who respond better to this postoperative problem. Strategies for timing of intervention in these patients necessarily involves echocardiographic evaluation, and some of the echocardiographic indices for PR include pressure half-time of the regurgitant jet, presence of flow reversal in the branch pulmonary arteries, and RV size and function [102]. Restrictive RV physiology can also be identified when diastolic forward flow is seen in the main pulmonary artery during atrial systole by Doppler interrogation [103]. Currently, cardiac MRI and its ability to quantitatively assess RV size and function have superseded echocardiography in determining the timing of intervention [104–106].

Intraoperative assessment of PR by TEE involves color mapping in midesophageal views along multiple planes such as the ME AoV SAX and ME RV In-Out views (Fig. 13.25, Video 13.24). Occasionally a somewhat higher esophageal view, such as the ME Asc Ao SAX and upper esophageal views (UE PA, UE Ao Arch SAX), can provide better color mapping display of the to-and-fro flow across the PV. These views can also display diastolic reversal in the proximal branch pulmonary arteries by color mapping and pulsed wave Doppler interrogation. The DTG RVOT view at 90° can also display the PR, especially since the direction of flow is parallel to the echocardiographic

beam. However, the distance from the probe to the RVOT often limits color mapping in this view for larger patients. Following implantation of a PV, the postoperative TEE examination should exclude residual PR in multiple mid-esophageal views and in the DTG RVOT view at 90°. The new PV, whether it is a mechanical prosthetic valve, a bioprosthetic valve, or part of a valved homograft, should also be evaluated in midesophageal views using multiple planes such as the ME RV In-Out and MV AoV LAX with slight leftward rotation of the probe. The deep transgastric views (DTG RVOT and DTG 5-Ch) can also be useful in evaluating the flow across the PV, both with color mapping and spectral Doppler interrogation.

Summary

This chapter discusses the common congenital defects affecting the RV and LV outflow tracts in both children and adults. While the semilunar valves are most commonly involved, pathology can occur at any level—subvalvar, valvar, supravalvar, or a combination of one or more levels. Stenosis and/or regurgitation at either or both outflow tracts can occur. Thus, a careful echocardiographic evaluation must be undertaken to define precisely the nature, location, and severity of the abnormality/abnormalities. For evaluation of the outflow tracts, TEE excels by providing excellent anatomic imaging and color mapping. It plays a vital role in the perioperative evaluation of outflow tract abnormalities with precise characterization of the pathology preoperatively and assessment of the adequacy of surgical repair postoperatively. It is also important in the evaluation of interventional procedures such as transcatheter pulmonary and AoV implantation. In addition, TEE can also be valuable in the ambulatory setting, such as the assessment of subaortic stenosis in older patients. Thus, for the assessment and treatment of outflow tract abnormalities, TEE serves as an important and extremely valuable tool.

Case-Based Examples

Case #1

Subject: Subaortic membrane.

Clinical History: A 5 year-old boy presents to the pediatric cardiology clinic for the evaluation of a cardiac murmur. The mother reports the history of a "hole in the heart" that has closed spontaneously. She reports that he has recently been unable to keep up with other children his age in kindergarten, yet denies syncope or presyncope. On physical examination, he is growing along the 50th percentile for height and weight, HR 92 bpm, BP 90/56 mmHg, RR 24 breath/min, oxygen saturation 99%. He has a normal S1 and S2. A Grade 3/6 low-pitched ejection systolic murmur is appreciated in the second and third left intercostal spaces, and radiates to the suprasternal notch. He has no clicks or gallops. He has normal and symmetric upper and lower extremity pulses.

After initial evaluation patient was referred for surgical repair and the following preoperative TEE images (Fig. 13.26, Videos 13.25 and 13.26) are shown.

TEE Findings:
Midesophageal long axis views of the aortic valve (~120°) show a discrete subaortic ridge located at the crest of the muscular septum, resulting in subaortic stenosis. Flow turbulence is seen starting at the level of the subaortic ridge on color mapping.

Discussion: Subvalvar aortic stenosis, also called subaortic stenosis, is a rare disorder seen in infants and children. In most cases, there is a membrane (usually muscular) just below the aortic valve, which causes a fixed obstruction to the blood flow across the left ventricular outflow tract. It can also be secondary to a fibromuscular ridge, a diffuse tunnel narrowing in the left ventricular outflow tract, or accessory

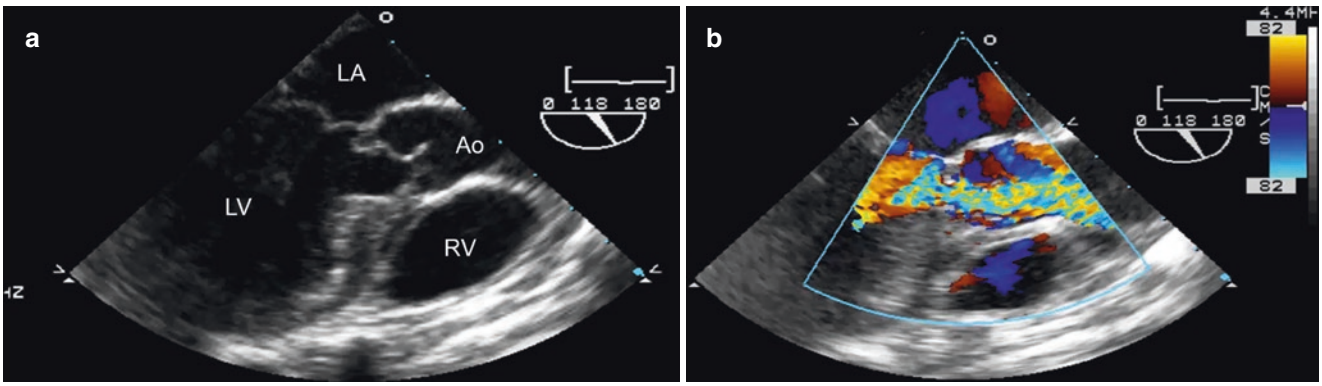

Fig. 13.26 **Case #1.** Subaortic stenosis seen from midesophageal aortic valve long axis view. (**a**) Shows two-dimensional image. (**b**) Shows turbulent color flow Doppler through the subaortic area. *Ao* aorta, *LA* left atrium, *LV* left ventricle, *RV* right ventricle. See text for details

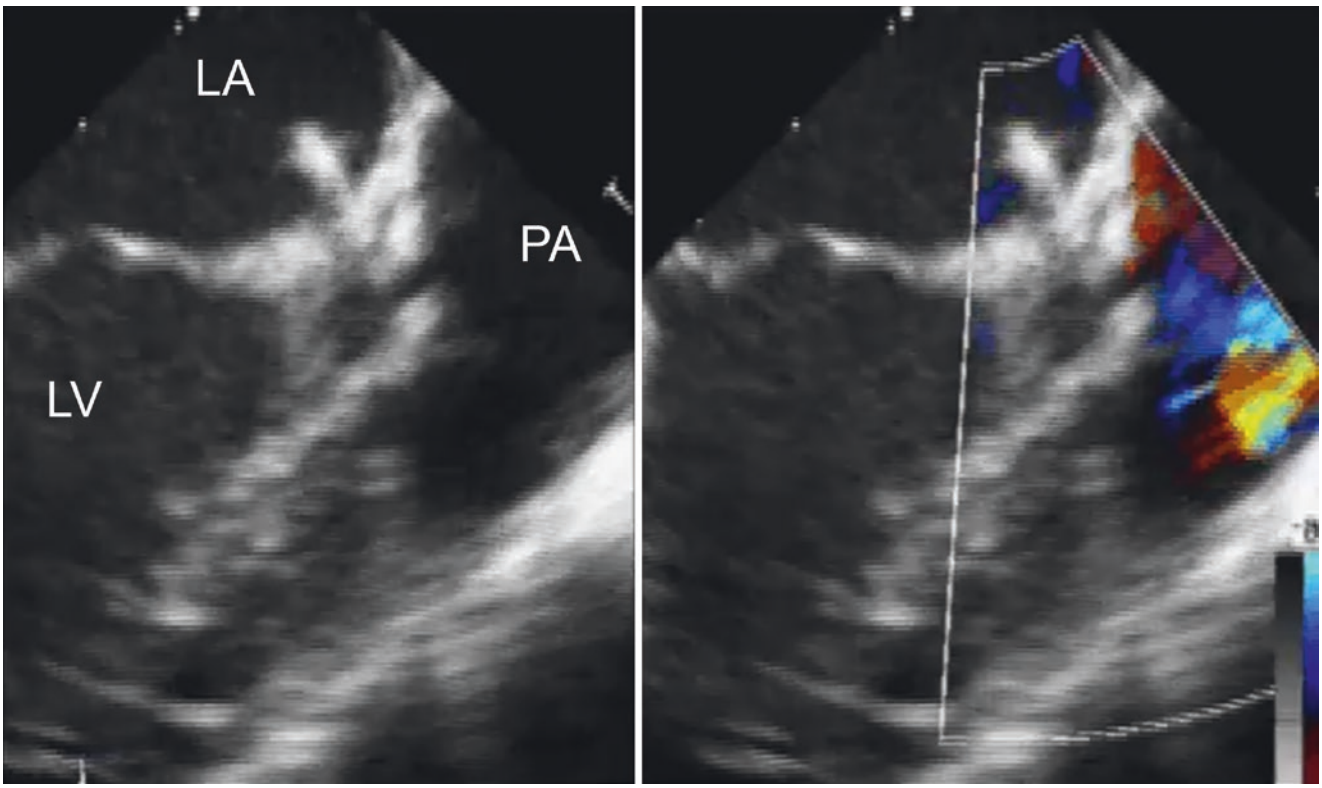

Fig. 13.27 **Case #2.** Valvar pulmonary stenosis seen from midesophageal aortic valve long axis view with transducer angle 90° and slight leftward probe rotation, showing the right ventricular outflow tract and turbulent flow across the pulmonary valve. *LA* left atrium, *LV* left ventricle, *PA* pulmonary artery. See text for details

mitral valve tissue. Congenital subaortic stenosis is rare, and progresses gradually. It is associated with a VSD, bicuspid aortic stenosis, double chamber right ventricle, and coarctation. It can result in aortic valve regurgitation. Management is surgical and depends on the type of subvalvar aortic resection. It can range from removal of the membrane to extensive ring resection, with or without ventricular septal myectomy. Discrete subaortic membranes have a high rate of postoperative recurrence.

Suggested Reading/References

1. Cilliers AM, Gewillig M. Rheology of discrete subaortic stenosis. Heart. 2002;88:335–6.
2. Sigfusson G, Tacy TA, Vanauker MD, Cape EG. Abnormalities of the left ventricular outflow tract associated with discrete subaortic stenosis in children: an echocardiographic study. J Am Coll Cardiol. 1997;30:255–9.
3. Stassano P, Di Tommaso L, Contaldo A, et al. Discrete subaortic stenosis: long-term prognosis on the progression of the obstruction and of the aortic insufficiency. Thorac Cardiovasc Surg. 2005; 53:23–7.
4. Mukadam S, Gordon BM, Olson JT, Newcombe JB, Hasaniya NW, Razzouk AJ, Bailey LL. Subaortic Stenosis Resection in Children: Emphasis on Recurrence and the Fate of the Aortic Valve. World J Pediatr Congenit Heart Surg. 2018 Sep;9(5):522–528.

Case #2

Subject: Pulmonary stenosis.

Clinical History: A 7-year-old girl presents with a secundum atrial septal defect and is found to have pulmonary stenosis on TEE imaging (Fig. 13.27, Video 13.27).

TEE Findings:
Midesophageal aortic valve long axis view with transducer angle 90° and slight leftward probe rotation, showing the RVOT. This video shows valvar pulmonary stenosis with thin but doming pulmonary valve leaflets, and post-stenotic dilation of the main pulmonary artery.

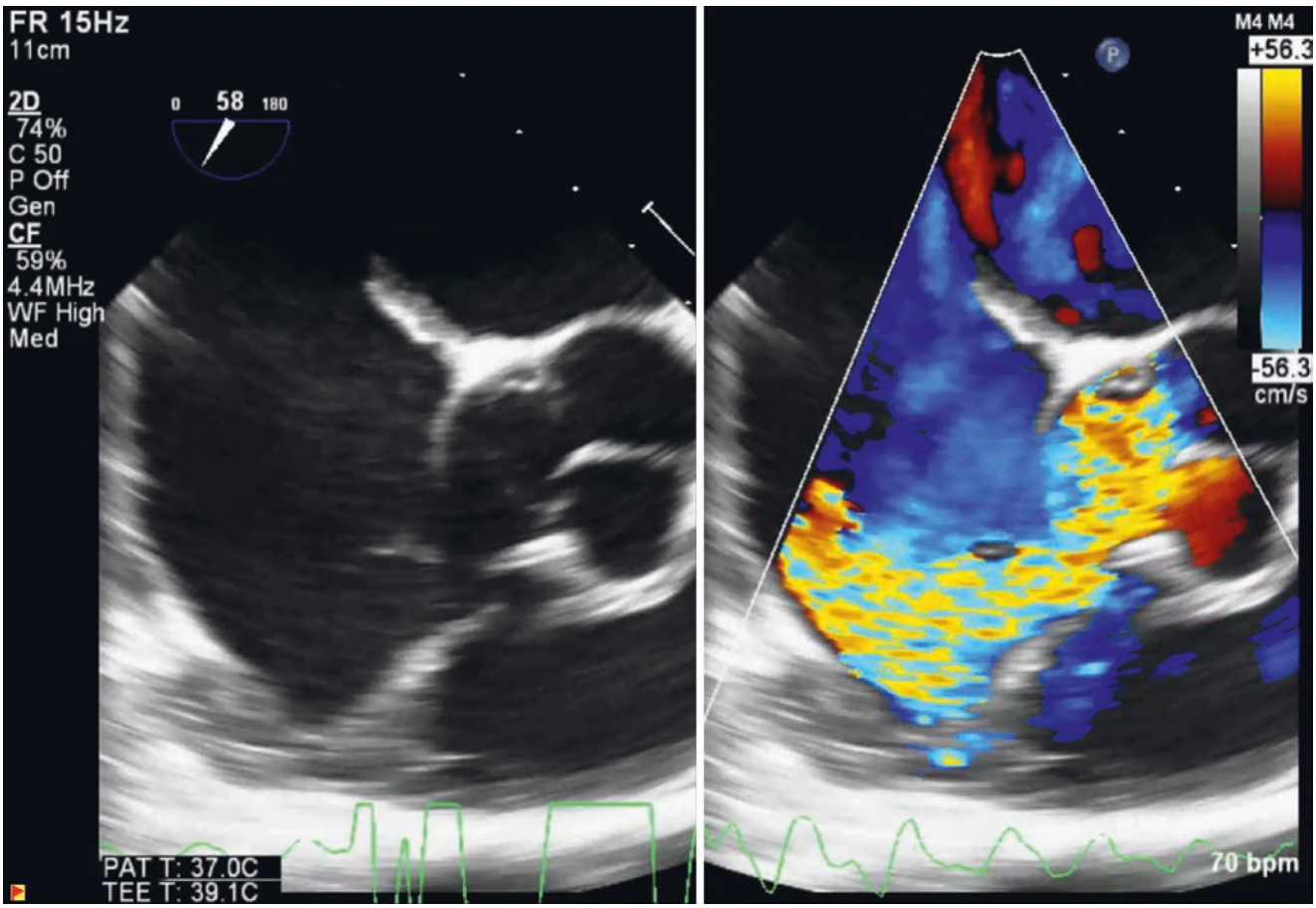

Fig. 13.28 Question #1. See Question for details

Discussion: Valvar pulmonary stenosis is one of the most commonly occurring congenital heart lesions (~10%). It can present as thin doming valve leaflets or as dysplastic leaflets. Most cases are treated by balloon valvotomy. TEE is rarely needed during balloon valvotomy unless, as in this case, it was needed for transcatheter atrial septal defect closure. Dysplastic valves are less amenable to balloon valvotomy and often require a surgical valvotomy, sometimes a partial pulmonary valvectomy, and possibly a transannular RVOT patch. The PV is best evaluated from the ME AoV SAX view, the ME RV In-Out view, and a modified ME AoV LAX view at 90° with leftward probe rotation to visualize the pulmonary outflow tract. Quantitative assessment of the degree of valvar PS can be performed in the DTG RVOT view at 90°.

Suggested Reading/References

1. Martinez RM, Anderson RH. Echocardiographic features of the morphologically right ventriculo-arterial junction. Cardiol Young. 2005;15 Suppl 1:17–26.
2. Stamm C, Anderson RH, Ho SY. Clinical anatomy of the normal pulmonary root compared with that in isolated pulmonary valvu-lar stenosis. J Am Coll Cardiol. 1998;31:1420–5.
3. Sommer RJ, Rhodes JF, Parness IA. Physiology of critical pulmonary valve obstruction in the neonate. Catheterization cardiovascular interventions. 2000;50:473–479

Table 13.1 reprinted from Zoghbi WA et al. [72], with permission from Elsevier

Questions and Answers

1. A 20 year old male patient presents with sudden onset of severe dyspnea, palpitations, and deterioration in exercise capacity. On admission a grade 4/6 continuous murmur is heard over the right midsternal border. A transthoracic echocardiogram was performed that showed a dilated right atrium and right ventricle and possible aortic regurgitation. The aortic valve was not well visualized. Based on the TEE images (Fig. 13.28, Video 13.28). What is the most likely diagnosis?
   a. Aortic regurgitation
   b. Left ventricular to aortic tunnel
   c. Left ventricular to right atrial shunt
   d. Ruptured sinus of Valsalva aneurysm

Answer: d

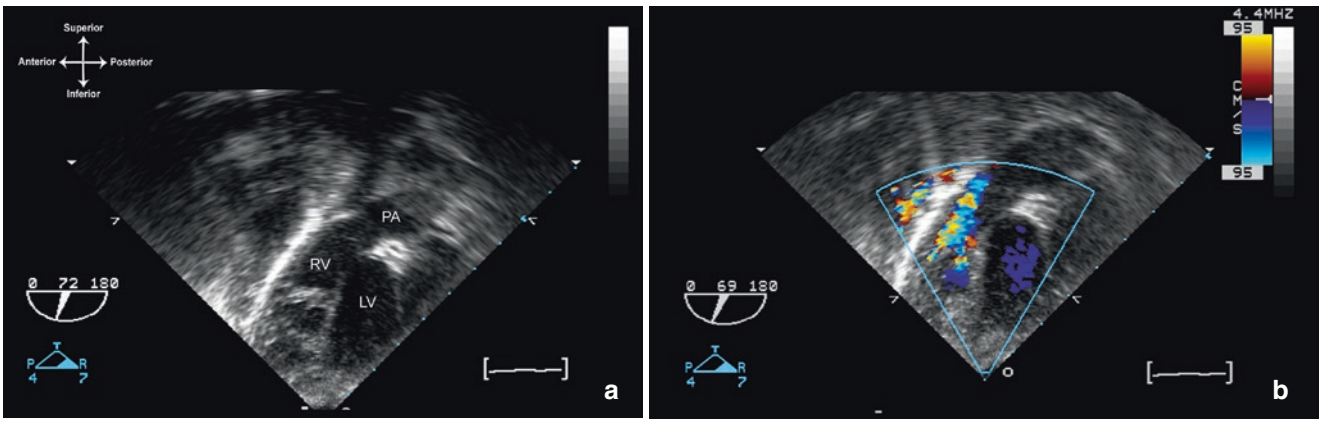

Fig. 13.29 (**a**, **b**) Question 2. See Question for details

Explanation: This is a midesophageal right ventricular inflow-outflow view (transducer angle 58°) showing a short axis view of the aortic valve and a ruptured non-coronary sinus of Valsalva aneurysm into the right atrium. Sinus of Valsalva aneurysm is a rare cardiac anomaly, and arises mainly from a congenital defect of the aortic media or may follow bacterial endocarditis. It occurs in between 0.09 and 0.15% of cases, and comprises up to 3.5% of all congenital cardiac anomalies. Coexisting cardiac lesions, especially a ventricular septal defect or aortic valve regurgitation, can be present in about 30 to 40% of patients. The aneurysms originate predominantly from the right coronary sinus (70%), and are more prevalent in males. Most aneurysms rupture into the right-sided heart chambers; rarely, they can rupture into the left-sided heart chambers, pericardium, and pulmonary artery or superior vena cava. Echocardiography, especially TEE, is important for diagnosing ruptured and non-ruptured aneurysms. It allows accurate evaluation of the involved sinus, the presence of a left-to-right shunt or associated cardiac lesions. Magnetic resonance imaging might be useful in diagnosing certain coexisting cardiac lesions more precisely. Cardiac catheterization is currently only performed to evaluate coronary anatomy prior to surgery. The optimal management for a ruptured sinus of Valsalva aneurysm is surgical repair.

2. A 15 year old male patient who recently immigrated to the United States presents with a murmur and a history of a ventricular septal defect surgically closed at 6 months of age.

On examination he has a heart rate of 80 bpm, blood pressure in the right upper extremity is 110/70 mmHg, respiratory rate is 18 breaths/mm and oxygen saturation is 98%. Cardiac auscultatory findings: S1 and S2 are normal without a loud pulmonary component or systolic click. A 5/6 systolic ejection murmur increasing with inspiration is present along the left mid-sternal border. Chest is clear. There is no hepatosplenomegaly. Extremities are warm and well perfused, there are easily palpable femoral pulses with no radial-femoral delay.

Based on the TEE images in Fig. 13.29 what is the most likely diagnosis:

a. Pulmonary stenosis
b. Double chamber right ventricle
c. Pulmonary hypertension
d. Tetralogy of Fallot

Answer: b

Explanation: This is a TEE deep transgastric RVOT view (transducer angle approximately 70°) showing a double chamber right ventricle with prominent muscle bundles at the infundibular os separating the proximal right ventricular chamber from the distal, well-developed right ventricular infundibular chamber, resulting in subvalvar pulmonary stenosis. Color flow Doppler demonstrates significant turbulence across the area. (*LV* left ventricle, PA main pulmonary artery, RV right ventricle).

3. A 5 year old girl was referred for surgical resection of a fibromuscular subaortic membrane that resulted in subaortic stenosis (peak pressure gradient 64 mmHg on transthoracic echocardiogram). She has moderate left ventricular hypertrophy and normal global systolic function. The preoperative TEE shows a fibromuscular ridge in the subaortic region with a peak pressure gradient ~40 mmHg.

What is the next best step?

a. Surgical resection of the subaortic membrane
b. Hold off surgical repair since the subaortic stenosis is not severe

c. Review the transthoracic echocardiogram findings at the next diagnostic error review session
d. Repeat the TEE while the patient is awake

Answer: a

Explanation: Based on the transthoracic echocardiogram findings, the patient qualifies for surgical resection. The discrepancy between the transthoracic echocardiogram and TEE is secondary to the alteration in the hemodynamic status of the patient after the administration of general anesthesia. The degree of left ventricular outflow tract obstruction can be difficult to assess by TEE, particularly in the operating room. It can be artificially decreased in the setting of general anesthesia, deep sedation, or hypovolemia.

4. What is the best TEE view to quantify the degree of residual left ventricular outflow tract obstruction post subvalvar aortic stenosis surgical repair
   a. Midesophageal aortic valve long axis (ME AoV LAX)
   b. Midesophageal ascending aorta (ME Asc Ao) views
   c. Deep transgastric five-chamber (DTG 5-Ch)
   d. Midesophageal aortic valve short axis (ME AoV SAX)

Answer: c

Explanation: The DTG 5-Ch views provides the best Doppler angle of interrogation for the left ventricular outflow tract, and is therefore the best of these choices for quantification of the degree of left ventricular outflow tract obstruction.

5. TEE is most valuable for the postoperative or post-intervention assessment of the following surgery/intervention:
   a. Ross procedure for aortic regurgitation
   b. Aortic valve balloon valvotomy for aortic stenosis
   c. Pulmonary valve balloon valvotomy for pulmonary stenosis
   d. Surgical end to end anastomosis of a coarctation

Answer: a

Explanation: TEE is most valuable for the postoperative evaluation of the Ross procedure, mainly for the following: evaluation of the pulmonary homograft for stenosis or regurgitation, assessment of the degree of neo-aortic valve regurgitation, and monitoring of ventricular function. TEE is rarely used in transcatheter aortic and pulmonary balloon valvotomy. In a coarctation the aortic isthmus (i.e. the region of interest) is generally not visualized completely by TEE. The adequacy of a coarctation repair can be performed by direct pressure measurements of the arch intraoperatively before and after the site of repair. Transthoracic echocardiography and cardiac MRI/CT are the imaging modalities used in the assessment of the arch after coarctation repair.

References

1. Hoffman JI, Kaplan S. The incidence of congenital heart disease. J Am Coll Cardiol. 2002;39(12):1890–900.
2. Triedman JK. Methodological issues for database development: trends. In: Keane JF, Fyler DC, Lock J, editors. Nadas' pediatric cardiology. 2nd ed. Philadelphia: Saunders; 2006. p. 323–36.
3. Campbell M. Calcific aortic stenosis and congenital bicuspid aortic valves. Br Heart J. 1968;30(5):606–16.
4. Roberts WC. The congenitally bicuspid aortic valve. A study of 85 autopsy cases. Am J Cardiol. 1970;26(1):72–83.
5. Ward C. Clinical significance of the bicuspid aortic valve. Heart. 2000;83(1):81–5.
6. Puchalski MD, Lui GK, Miller-Hance WC, Brook MM, Young LT, Bhat A, et al. Guidelines for performing a comprehensive transesophageal echocardiographic examination in children and all patients with congenital heart disease: recommendations from the American Society of Echocardiography. J Am Soc Echocardiogr. 2019;32(2):173–215.
7. Kaushal SK, Radhakrishanan S, Dagar KS, Iyer PU, Girotra S, Shrivastava S, et al. Significant intraoperative right ventricular outflow gradients after repair for tetralogy of Fallot: to revise or not to revise? Ann Thorac Surg. 1999;68(5):1705–12. discussion 12–3
8. Anderson RH, Freedom RM. Normal and abnormal structure of the ventriculo-arterial junctions. Cardiol Young. 2005;15(Suppl 1):3–16.
9. Dare AJ, Veinot JP, Edwards WD, Tazelaar HD, Schaff HV. New observations on the etiology of aortic valve disease: a surgical pathologic study of 236 cases from 1990. Hum Pathol. 1993;24(12):1330–8.
10. Angelini A, Ho SY, Anderson RH, Devine WA, Zuberbuhler JR, Becker AE, et al. The morphology of the normal aortic valve as compared with the aortic valve having two leaflets. J Thorac Cardiovasc Surg. 1989;98(3):362–7.
11. Fernandes SM, Sanders SP, Khairy P, Jenkins KJ, Gauvreau K, Lang P, et al. Morphology of bicuspid aortic valve in children and adolescents. J Am Coll Cardiol. 2004;44(8):1648–51.
12. Beppu S, Suzuki S, Matsuda H, Ohmori F, Nagata S, Miyatake K. Rapidity of progression of aortic stenosis in patients with congenital bicuspid aortic valves. Am J Cardiol. 1993;71(4):322–7.
13. Fernandes SM, Khairy P, Sanders SP, Colan SD. Bicuspid aortic valve morphology and interventions in the young. J Am Coll Cardiol. 2007;49(22):2211–4.
14. Miller MJ, Geffner ME, Lippe BM, Itami RM, Kaplan SA, DiSessa TG, et al. Echocardiography reveals a high incidence of bicuspid aortic valve in turner syndrome. J Pediatr. 1983;102(1):47–50.
15. Fedak PW, Verma S, David TE, Leask RL, Weisel RD, Butany J. Clinical and pathophysiological implications of a bicuspid aortic valve. Circulation. 2002;106(8):900–4.
16. Nistri S, Sorbo MD, Basso C, Thiene G. Bicuspid aortic valve: abnormal aortic elastic properties. J Heart Valve Dis. 2002;11(3):369–73. discussion 73-4
17. Nkomo VT, Enriquez-Sarano M, Ammash NM, Melton L Jr, Bailey KR, Desjardins V, et al. Bicuspid aortic valve associated with aortic dilatation: a community-based study. Arterioscler Thromb Vasc Biol. 2003;23(2):351–6.
18. Wagner HR, Ellison RC, Keane JF, Humphries OJ, Nadas AS. Clinical course in aortic stenosis. Circulation. 1977;56(1 Suppl):I47–56.
19. Keane JF, Driscoll DJ, Gersony WM, Hayes CJ, Kidd L, O'Fallon WM, et al. Second natural history study of congenital heart defects. Results of treatment of patients with aortic valvar stenosis. Circulation. 1993;87(2 Suppl):I16–27.

20. Savino JS. Transesophageal echocardiographic evaluation of native valvular disease and repair. Crit Care Clin. 1996;12(2):321–81.
21. Mehta Y, Singh R. Quantification of AS and AR. Ann Card Anaesth. 2009;12(2):166.
22. Nishimura RA, Otto CM, Bonow RO, Carabello BA, Erwin JP 3rd, Guyton RA, et al. 2014 AHA/ACC guideline for the management of patients with valvular heart disease: a report of the American College of Cardiology/American Heart Association task force on practice guidelines. J Am Coll Cardiol. 2014;63(22):e57–185.
23. Heinrich RS, Fontaine AA, Grimes RY, Sidhaye A, Yang S, Moore KE, et al. Experimental analysis of fluid mechanical energy losses in aortic valve stenosis: importance of pressure recovery. Ann Biomed Eng. 1996;24(6):685–94.
24. Baumgartner H, Hung J, Bermejo J, Chambers JB, Evangelista A, Griffin BP, et al. Echocardiographic assessment of valve stenosis: EAE/ASE recommendations for clinical practice. J Am Soc Echocardiogr. 2009;22(1):1–23. quiz 101-2
25. Nakai H, Takeuchi M, Yoshitani H, Kaku K, Haruki N, Otsuji Y. Pitfalls of anatomical aortic valve area measurements using two-dimensional transoesophageal echocardiography and the potential of three-dimensional transoesophageal echocardiography. Eur J Echocardiogr. 2010;11(4):369–76.
26. Schneider DJ, Moore JW. Aortic stenosis. In: Allen HD, Driscoll DJ, Shaddy RE, Feltes TF, editors. Moss and Adams' heart disease in infants, children, and adolescents: including the fetus and young adult. 7th ed. Philadelphia: Lippincott Williams & Wilkins; 2008. p. 968–87.
27. Simpson JM. Anomalies of left ventricular outflow tract and aortic valve. In: Lai W, Mertens L, Cohen MS, Geva T, editors. Echocardiography in pediatric and congenital heart disease: from fetus to adult. Illustrated ed. Hoboken, NJ: Wiley; 2009. p. 297–314.
28. Lopez L. Abnormalities of left ventricular outflow. In: Eidem BW, Ceteta F, O'Leary PW, editors. Echocardiography in pediatric and adult congenital heart disease. Philadelphia, PA: Lippincott Williams & Wilkins; 2010. p. 215–36.
29. Lopez L, Colan SD, Frommelt PC, Ensing GJ, Kendall K, Younoszai AK, et al. Recommendations for quantification methods during the performance of a pediatric echocardiogram: a report from the Pediatric Measurements Writing Group of the American Society of Echocardiography Pediatric and Congenital Heart Disease Council. J Am Soc Echocardiogr. 2010;23(5):465–95. quiz 576-7
30. Daubeney PE, Blackstone EH, Weintraub RG, Slavik Z, Scanlon J, Webber SA. Relationship of the dimension of cardiac structures to body size: an echocardiographic study in normal infants and children. Cardiol Young. 1999;9(4):402–10.
31. Pettersen MD, Du W, Skeens ME, Humes RA. Regression equations for calculation of z scores of cardiac structures in a large cohort of healthy infants, children, and adolescents: an echocardiographic study. J Am Soc Echocardiogr. 2008;21(8):922–34.
32. Leon MB, Smith CR, Mack M, Miller DC, Moses JW, Svensson LG, et al. Transcatheter aortic-valve implantation for aortic stenosis in patients who cannot undergo surgery. N Engl J Me. 2010;363(17):1597–607.
33. Rotman OM, Bianchi M, Ghosh RP, Kovarovic B, Bluestein D. Principles of TAVR valve design, modelling, and testing. Expert Rev Med Devices. 2018;15(11):771–91.
34. Billings FT, Kodali SK, Shanewise JS. Transcatheter aortic valve implantation: anesthetic considerations. Anesth Analg. 2009;108(5):1453–62.
35. Abdel-Wahab M, Mehilli J, Frerker C, Neumann FJ, Kurz T, Tolg R, et al. Comparison of balloon-expandable vs self-expandable valves in patients undergoing transcatheter aortic valve replacement: the CHOICE randomized clinical trial. JAMA. 2014;311(15):1503–14.
36. Gilard M, Eltchaninoff H, Iung B, Donzeau-Gouge P, Chevreul K, Fajadet J, et al. Registry of transcatheter aortic-valve implantation in high-risk patients. N Engl J Med. 2012;366(18):1705–15.
37. Makkar RR, Fontana GP, Jilaihawi H, Kapadia S, Pichard AD, Douglas PS, et al. Transcatheter aortic-valve replacement for inoperable severe aortic stenosis. N Engl J Med. 2012;366(18):1696–704.
38. Thyregod HGH, Steinbrüchel DA, Ihlemann N, Nissen H, Kjeldsen BJ, Petursson P, et al. Transcatheter versus surgical aortic valve replacement in patients with severe aortic valve stenosis: 1-year results from the all-comers NOTION randomized clinical trial. J Am Coll Cardiol. 2015;65(20):2184–94.
39. Mack MJ, Leon MB, Thourani VH, Makkar R, Kodali SK, Russo M, et al. Transcatheter aortic-valve replacement with a balloon-expandable valve in low-risk patients. N Engl J Med. 2019;380(18):1695–705.
40. Leichter DA, Sullivan I, Gersony WM. "acquired" discrete subvalvular aortic stenosis: natural history and hemodynamics. J Am Coll Cardiol. 1989;14(6):1539–44.
41. Vogt J, Dische R, Rupprath G, de Vivie ER, Kotthoff S, Kececioglu D. Fixed subaortic stenosis: an acquired secondary obstruction? A twenty-seven year experience with 168 patients. Thorac Cardiovasc Surg. 1989;37(4):199–206.
42. Cape EG, Vanauker MD, Sigfusson G, Tacy TA, del Nido PJ. Potential role of mechanical stress in the etiology of pediatric heart disease: septal shear stress in subaortic stenosis. J Am Coll Cardiol. 1997;30(1):247–54.
43. Cilliers AM, Gewillig M. Rheology of discrete subaortic stenosis. Heart. 2002;88(4):335–6.
44. Kleinert S, Geva T. Echocardiographic morphometry and geometry of the left ventricular outflow tract in fixed subaortic stenosis. J Am Coll Cardiol. 1993;22(5):1501–8.
45. Sigfusson G, Tacy TA, Vanauker MD, Cape EG. Abnormalities of the left ventricular outflow tract associated with discrete subaortic stenosis in children: an echocardiographic study. J Am Coll Cardiol. 1997;30(1):255–9.
46. Bezold LI, Smith EO, Kelly K, Colan SD, Gauvreau K, Geva T. Development and validation of an echocardiographic model for predicting progression of discrete subaortic stenosis in children. Am J Cardiol. 1998;81(3):314–20.
47. Melero JM, Rodriguez I, Such M, Porras C, Olalla E. Left ventricular outflow tract obstruction with mitral mechanical prosthesis. Ann Thorac Surg. 1999;68(1):255–7.
48. Rietman GW, van der Maaten JMAA, Douglas YL, Boonstra PW. Echocardiographic diagnosis of left ventricular outflow tract obstruction after mitral valve replacement with subvalvular preservation. Eur J Cardiothorac Surg. 2002;22(5):825–7.
49. Wu Q, Zhang L, Zhu R. Obstruction of left ventricular outflow tract after mechanical mitral valve replacement. Ann Thorac Surg. 2008;85(5):1789–91.
50. Geva T, Hornberger LK, Sanders SP, Jonas RA, Ott DA, Colan SD. Echocardiographic predictors of left ventricular outflow tract obstruction after repair of interrupted aortic arch. J Am Coll Cardiol. 1993;22(7):1953–60.
51. Salem MM, Starnes VA, Wells WJ, Acherman RJ, Chang RK, Luciani GB, et al. Predictors of left ventricular outflow obstruction following single-stage repair of interrupted aortic arch and ventricular septal defect. Am J Cardiol. 2000;86(9):1044–7.
52. Silverman NH, Gerlis LM, Ho SY, Anderson RH. Fibrous obstruction within the left ventricular outflow tract associated with ventricular septal defect: a pathologic study. J Am Coll Cardiol. 1995;25(2):475–81.
53. Vogel M, Smallhorn JF, Freedom RM, Coles J, Williams WG, Trusler GA. An echocardiographic study of the association of ventricular septal defect and right ventricular muscle bundles with a fixed subaortic abnormality. Am J Cardiol. 1988;61(10):857–60.

54. Coleman DM, Smallhorn JF, McCrindle BW, Williams WG, Freedom RM. Postoperative follow-up of fibromuscular subaortic stenosis. J Am Coll Cardiol. 1994;24(6):1558–64.
55. Oliver JM, Gonzalez A, Gallego P, Sanchez-Recalde A, Benito F, Mesa JM. Discrete subaortic stenosis in adults: increased prevalence and slow rate of progression of the obstruction and aortic regurgitation. J Am Coll Cardiol. 2001;38(3):835–42.
56. Stassano P, Di Tommaso L, Contaldo A, Monaco M, Mottola M, Musumeci A, et al. Discrete subaortic stenosis: long-term prognosis on the progression of the obstruction and of the aortic insufficiency. Thorac Cardiovasc Surg. 2005;53(1):23–7.
57. Kuralay E, Ozal E, Bingol H, Cingoz F, Tatar H. Discrete subaortic stenosis: assessing adequacy of myectomy by transesophageal echocardiography. J Card Surg. 1999;14(5):348–53.
58. Darcin OT, Yagdi T, Atay Y, Engin C, Levent E, Buket S, et al. Discrete subaortic stenosis: surgical outcomes and follow-up results. Tex Heart Inst J. 2003;30(4):286–92.
59. Mukadam S, Gordon BM, Olson JT, Newcombe JB, Hasaniya NW, Razzouk AJ, et al. Subaortic stenosis resection in children: emphasis on recurrence and the fate of the aortic valve. World J Pediatr Congenit Heart Surg. 2018;9(5):522–8.
60. Bernhard WF, Keane JF, Fellows KE, Litwin SB, Gross RE. Progress and problems in the surgical management of congenital aortic stenosis. J Thorac Cardiovasc Surg. 1973;66(3):404–19.
61. Williams JCP, Barratt-Boyes BG, Lowe JB. Supravalvular Aortic Stenosis. Circulation. 1961;24(6):1311–8.
62. Brooke BS, Bayes-Genis A, Li DY. New insights into elastin and vascular disease. Trends Cardiovasc Med. 2003;13(5):176–81.
63. Ewart AK, Jin W, Atkinson D, Morris CA, Keating MT. Supravalvular aortic stenosis associated with a deletion disrupting the elastin gene. J Clin Invest. 1994;93(3):1071–7.
64. O'Connor WN, Davis JB, Geissler R, Cottrill CM, Noonan JA, Todd EP. Supravalvular aortic stenosis. Clinical and pathologic observations in six patients. Arch Pathol Lab Med. 1985;109(2):179–85.
65. Stamm C, Li J, Ho SY, Redington AN, Anderson RH. The aortic root in supravalvular aortic stenosis: the potential surgical relevance of morphologic findings. J Thorac Cardiovasc Surg. 1997;114(1):16–24.
66. Firstenberg MS, Greenberg NL, Lin SS, Garcia MJ, Alexander LA, Thomas JD. Transesophageal echocardiography assessment of severe ostial left main coronary stenosis. J Am Soc Echocardiogr. 2000;13(7):696–8.
67. Jureidini SB, Marino CJ, Singh GK, Fiore A, Balfour IC. Main coronary artery and coronary ostial stenosis in children: detection by transthoracic color flow and pulsed Doppler echocardiography. J Am Soc Echocardiogr. 2000;13(4):255–63.
68. Sobkowicz B, Hirnle T, Dobrzycki S, Frank M, Sawicki R. Intraoperative echocardiographic assessment of the severe isolated ostial stenosis of left main coronary artery before and after surgical patch angioplasty. Eur J Echocardiogr. 2005;6(4):280–5.
69. Donofrio MT, Engle MA, O'Loughlin JE, Snyder MS, Levin AR, Ehlers KH, et al. Congenital aortic regurgitation: natural history and management. J Am Coll Cardiol. 1992;20(2):366–72.
70. Enriquez-Sarano M, Tajik AJ. Clinical practice. Aortic regurgitation. N Engl J Med. 2004;351(15):1539–46.
71. Tweddell JS, Pelech AN, Frommelt PC, Jaquiss RDB, Hoffman GM, Mussatto KA, et al. Complex aortic valve repair as a durable and effective alternative to valve replacement in children with aortic valve disease. J Thorac Cardiovasc Surg. 2005;129(3):551–8.
72. Zoghbi WA, Adams D, Bonow RO, Enriquez-Sarano M, Foster E, Grayburn PA, et al. Recommendations for noninvasive evaluation of native valvular regurgitation: a report from the American Society of Echocardiography developed in collaboration with the Society for Cardiovascular Magnetic Resonance. J Am Soc Echocardiogr. 2017;30(4):303–71.
73. Lancellotti P, Tribouilloy C, Hagendorff A, Moura L, Popescu BA, Agricola E, et al. European Association of Echocardiography recommendations for the assessment of valvular regurgitation. Part 1: aortic and pulmonary regurgitation (native valve disease). Eur J Echocardiogr. 2010;11(3):223–44.
74. Friedrich AD, Shekar PS. Interrogation of the aortic valve. Crit Care Med. 2007;35(8 Suppl):S365–71.
75. Tribouilloy CM, Enriquez-Sarano M, Fett SL, Bailey KR, Seward JB, Tajik AJ. Application of the proximal flow convergence method to calculate the effective regurgitant orifice area in aortic regurgitation. J Am Coll Cardiol. 1998;32(4):1032–9.
76. Honjo O, Kotani Y, Osaki S, Fujita Y, Suezawa T, Tateishi A, et al. Discrepancy between intraoperative transesophageal echocardiography and postoperative transthoracic echocardiography in assessing congenital valve surgery. Ann Thorac Surg. 2006;82(6):2240–6.
77. Tweddell JS, Pelech AN, Jaquiss RDB, Frommelt PC, Mussatto KA, Hoffman GM, et al. Aortic valve repair. Semin Thorac Cardiovasc Surg Pediatr Card Surg Annu. 2005;5:112–21.
78. Stern KWD, White MT, Verghese GR, Del Nido PJ, Geva T. Intraoperative echocardiography for congenital aortic valve repair: predictors of early reoperation. Ann Thorac Surg. 2015;100(2):678–85.
79. Marino BS, Pasquali SK, Wernovsky G, Pudusseri A, Rychik J, Montenegro L, et al. Accuracy of intraoperative transesophageal echocardiography in the prediction of future neo-aortic valve function after the Ross procedure in children and young adults. Congenit Heart Dis. 2008;3(1):39–46.
80. Dietz HC, Pyeritz RE, Hall BD, Cadle RG, Hamosh A, Schwartz J, et al. The Marfan syndrome locus: confirmation of assignment to chromosome 15 and identification of tightly linked markers at 15q15-q21.3. Genomics. 1991;9(2):355–61.
81. Boileau C, Jondeau G, Mizuguchi T, Matsumoto N. Molecular genetics of Marfan syndrome. Curr Opin Cardiol. 2005;20(3):194–200.
82. Yetman AT, Graham T. The dilated aorta in patients with congenital cardiac defects. J Am Coll Cardiol. 2009;53(6):461–7.
83. Abe T, Komatsu S. Surgical repair and long-term results in ruptured sinus of Valsalva aneurysm. Ann Thorac Surg. 1988;46(5):520–5.
84. Davies RR, Goldstein LJ, Coady MA, Tittle SL, Rizzo JA, Kopf GS, et al. Yearly rupture or dissection rates for thoracic aortic aneurysms: simple prediction based on size. Ann Thorac Surg. 2002;73(1):17–27. discussion-8
85. Thenabadu PN, Steiner RE, Cleland WP, Goodwin JF. Observations on the treatment of dissection of the aorta. Postgrad Med J. 1976;52(613):671–7.
86. Martinez RM, Anderson RH. Echocardiographic features of the morphologically right ventriculo-arterial junction. Cardiol Young. 2005;15(Suppl 1):17–26.
87. Stamm C, Anderson RH, Ho SY. Clinical anatomy of the normal pulmonary root compared with that in isolated pulmonary valvular stenosis. J Am Coll Cardiol. 1998;31(6):1420–5.
88. Roberts WC, Shemin RJ, Kent KM. Frequency and direction of interatrial shunting in valvular pulmonic stenosis with intact ventricular septum and without left ventricular inflow or outflow obstruction. An analysis of 127 patients treated by valvulotomy. Am Heart J. 1980;99(2):142–8.
89. Freedom RM, Yoo SJ. The divided right ventricle. In: Freedom RM, Yoo SJ, Mikailian H, Williams WG, editors. The natural and modified history of congenital heart disease. London: Wiley Online Library; 2004. p. 232–5.
90. Restivo A, Cameron AH, Anderson RH, Allwork SP. Divided right ventricle: a review of its anatomical varieties. Pediatr Cardiol. 1984;5(3):197–204.

91. Pongiglione G, Freedom RM, Cook D, Rowe RD. Mechanism of acquired right ventricular outflow tract obstruction in patients with ventricular septal defect: an angiocardiographic study. Am J Cardiol. 1982;50(4):776–80.
92. Wong PC, Sanders SP, Jonas RA, Colan SD, Parness IA, Geva T, et al. Pulmonary valve-moderator band distance and association with development of double-chambered right ventricle. Am J Cardiol. 1991;68(17):1681–6.
93. Lucas RV Jr, Varco RL, Lillehei CW, Adams P Jr, Anderson RC, Edwards JE. Anomalous muscle bundle of the right ventricle. Hemodynamic consequences and surgical considerations. Circulation. 1962;25:443–55.
94. Hachiro Y, Takagi N, Koyanagi T, Morikawa M, Abe T. Repair of double-chambered right ventricle: surgical results and long-term follow-up. Ann Thorac Surg. 2001;72(5):1520–2.
95. Simpson WF, Sade RM, Crawford FA, Taylor AB, Fyfe DA. Double-chambered right ventricle. Ann Thorac Surg. 1987;44(1):7–10.
96. McElhinney DB, Chatterjee KM, Reddy VM. Double-chambered right ventricle presenting in adulthood. Ann Thorac Surg. 2000;70(1):124–7.
97. Yoshida K, Yoshikawa J, Shakudo M, Akasaka T, Jyo Y, Takao S, et al. Color Doppler evaluation of valvular regurgitation in normal subjects. Circulation. 1988;78(4):840–7.
98. Keane JF, Fyler DC. Pulmonary stenosis. In: Keane JF, Fyler DC, Lock J, editors. Nadas' pediatric cardiology. 2nd ed. Philadelphia: Saunders; 2006. p. 549–58.
99. Veldtman GR, Dearani JA, Warnes CA. Low pressure giant pulmonary artery aneurysms in the adult: natural history and management strategies. Heart. 2003;89(9):1067–70.
100. Sayger P, Lewis M, Arcilla R, Ilbawi M. Isolated congenital absence of a single pulmonary valve cusp. Pediatr Cardiol. 2000;21(5):487–9.
101. Mercer-Rosa L, Yang W, Kutty S, Rychik J, Fogel M, Goldmuntz E. Quantifying pulmonary regurgitation and right ventricular function in surgically repaired tetralogy of Fallot: a comparative analysis of echocardiography and magnetic resonance imaging. Circ Cardiovasc Imaging. 2012;5(5):637–43.
102. Bouzas B, Chang AC, Gatzoulis MA. Pulmonary insufficiency: preparing the patient with ventricular dysfunction for surgery. Cardiol Young. 2005;15(Suppl 1):51–7.
103. Gatzoulis MA, Clark AL, Cullen S, Newman CG, Redington AN. Right ventricular diastolic function 15 to 35 years after repair of tetralogy of Fallot. Restrictive physiology predicts superior exercise performance. Circulation. 1995;91(6):1775–81.
104. Bouzas B, Kilner PJ, Gatzoulis MA. Pulmonary regurgitation: not a benign lesion. Eur Heart J. 2005;26(5):433–9.
105. Oosterhof T, van Straten A, Vliegen HW, Meijboom FJ, van Dijk APJ, Spijkerboer AM, et al. Preoperative thresholds for pulmonary valve replacement in patients with corrected tetralogy of Fallot using cardiovascular magnetic resonance. Circulation. 2007;116(5):545–51.
106. Geva T. Repaired tetralogy of Fallot: the roles of cardiovascular magnetic resonance in evaluating pathophysiology and for pulmonary valve replacement decision support. J Cardiovasc Magn Reson. 2011;13(9):9.